Pure Appl. Chem., Vol. 81, No. 5, pp. 791–828, 2009.
doi: 10.1351/PAC-REP-08-09-22

INTERNATIONAL UNION OF PURE AND APPLIED CHEMISTRY

PHYSICAL AND BIOPHYSICAL CHEMISTRY DIVISION*

THERMODYNAMIC AND THERMOPHYSICAL PROPERTIES OF THE REFERENCE IONIC LIQUID: 1-HEXYL-3-METHYLIMIDAZOLIUM BIS[(TRIFLUOROMETHYL)SULFONYL]AMIDE (INCLUDING MIXTURES). PART 2. CRITICAL EVALUATION AND RECOMMENDED PROPERTY VALUES

(IUPAC Technical Report)

Prepared for publication by
ROBERT D. CHIRICO[1,‡], VLADIMIR DIKY[1], JOSEPH W. MAGEE[1], MICHAEL FRENKEL[1], AND KENNETH N. MARSH[2]

[1]Thermophysical Properties Division, National Institute of Standards and Technology, Boulder, CO 80305-3328, USA; [2]Department of Chemical and Process Engineering, University of Canterbury, Private Bag 4800, Christchurch, New Zealand

‡Corresponding author

Thermodynamic and thermophysical properties of the reference ionic liquid: 1-hexyl-3-methylimidazolium bis[(trifluoromethyl)sulfonyl]amide (including mixtures). Part 2. Critical evaluation and recommended property values

(IUPAC Technical Report)

Abstract: This article is a product of IUPAC Project 2002-005-1-100 (Thermodynamics of ionic liquids, ionic liquid mixtures, and the development of standardized systems). Experimental results of thermodynamic, transport, and phase equilibrium studies made on a reference sample of the ionic liquid 1-hexyl-3-methylimidazolium bis[(trifluoromethyl)sulfonyl]amide are summarized, compared, and critically evaluated to provide recommended values with uncertainties for the properties measured. Properties measured included thermal properties (triple-point temperature, glass-transition temperature, enthalpy of fusion, heat capacities of condensed states), volumetric properties, speeds of sound, viscosities, electrolytic conductivities, relative permittivities, as well as properties for mixtures, such as gas solubilities (solubility pressures), solute activity coefficients at infinite dilution, and liquid–liquid equilibrium temperatures. Recommended values with uncertainties are provided for the properties studied experimentally. The effect of the presence of water on the property values is discussed.

Keywords: thermodynamic properties; transport properties; recommended values; critical evaluation; ionic liquids; IUPAC Physical and Biophysical Chemistry Division.

INTRODUCTION

This article is a product of IUPAC Project 2002-005-1-100 (Thermodynamics of ionic liquids, ionic liquid mixtures, and the development of standardized systems) chaired by Kenneth N. Marsh (University of Canterbury, Christchurch, New Zealand). Members of the project task group were Joan F. Brennecke (University of Notre Dame, Notre Dame, Indiana, USA), Michael Frenkel (National Institute of Standards and Technology, Boulder, Colorado, USA), Andreas Heintz (University of Rostock, Rostock, Germany), Joseph W. Magee (National Institute of Standards and Technology, Boulder, Colorado, USA), Cor J. Peters (Delft University of Technology, Delft, Netherlands), Luis Paulo N. Rebelo (Universidade Nova de Lisboa, Oeiras, Portugal), and Kenneth R. Seddon (the Queen's University of Belfast, Belfast, Northern Ireland, UK). The proposal for the project was also endorsed and approved by the International Association of Chemical Thermodynamics (IACT) [1].

Ionic liquids represent a class of liquid solvents having some characteristics of molten salts and are moisture-, air-, and temperature-stable with melting temperatures often below or near room temperature. Many ionic liquids consist of cations based on alkylimidazolium or alkylpyridinium ions and anions such as tetrafluoroborate, hexafluorophosphate, bis[(trifluoromethyl)sulfonyl]amide, tri-

fluoromethanesulfonate, and many others. The large number of possible ionic combinations allows for the possibility of designing compounds with specific properties.

Ionic liquids have attracted considerable interest during the last few years as new industrial solvents. They have very low vapor pressures and, therefore, exhibit favorable solvent properties for new homogeneous catalytic reactions and other chemical production processes. An increasing number of successful applications are described in the literature. The utilization of ionic liquids in industrial chemistry requires a systematic study of their thermodynamic, transport, and phase equilibria properties that are required for chemical process design. An extensive review of the field of ionic liquids was published recently [2].

Two objectives of the project were (1) to recommend a reference ionic liquid and make reference-quality measurements on selected thermophysical properties of both the pure ionic liquid and its mixtures, and (2) to establish recommended values for the properties measured and provide recommendations on measurement methods. The first of these objectives was completed, and the results of the reference-quality measurements have been published in the open literature. The present article describes the generation of recommended values for the wide variety of properties measured, including thermal properties (triple-point temperature, glass-transition temperature, enthalpy of fusion, heat capacities of condensed states), volumetric properties, speeds of sound, viscosities, electrolytic conductivities, as well as mixture properties, such as gas solubilities, solute activity coefficients at infinite dilution, and liquid–liquid equilibrium temperatures. A discussion of the experimental methods with recommendations is published separately [3].

A reference ionic liquid, 1-hexyl-3-methylimidazolium bis[(trifluoromethyl)sulfonyl]amide (abbreviation: $[C_6mim][NTf_2]$; see Fig. 1), was selected, synthesized, and purified, and its purity was fully characterized by members of the project team. This sample (termed the "IUPAC" sample here) was distributed to laboratories worldwide for completion of an extensive variety of thermodynamic, transport, and phase equilibrium measurements involving both the pure compound and mixtures with a second component. The present article provides a compilation of all experimental measurements to date on $[C_6mim][NTf_2]$, including those done with samples other than the IUPAC sample. Where possible, a critical evaluation of the available property measurements is made and recommended values with uncertainties are provided.

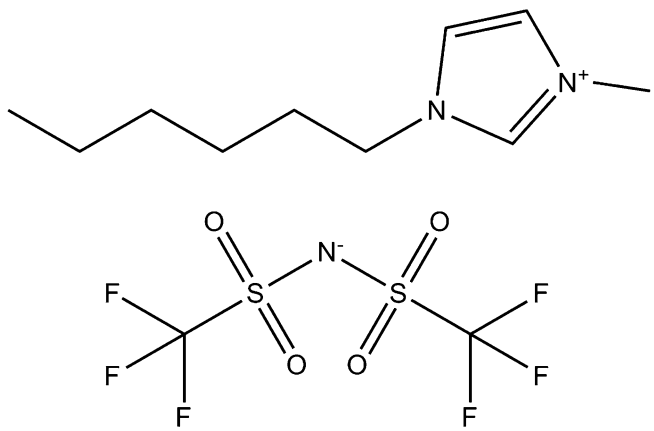

Fig. 1 The component ions of the ionic liquid 1-hexyl-3-methylimidazolium bis[(trifluoromethyl)sulfonyl]amide (abbreviation: $[C_6mim][NTf_2]$).

Results of the measurements on the IUPAC sample were published by the experimentalists in 21 journal articles and reports that are publicly available. Some property values are published with the separate discussion of experimental methods [3]. All results are combined and compared here, and recommended values and equations for each measured property are provided. Other measurements reported in the literature (approximately 26 additional articles) for $[C_6mim][NTf_2]$ were considered, but generally, were not included in the evaluation process. Full bibliographic information for the measurements is given later in this report. Results obtained with the IUPAC sample are clearly indicated in all tables and figures.

SYNTHESIS AND CHARACTERIZATION OF THE IUPAC SAMPLE

A major impetus for this project was the existence of serious disagreements in the literature between property values measured independently for the same nominal ionic liquid. Subsequent research demonstrated that measured properties of ionic liquids were sensitive to the presence of relatively small amounts of water. (See [4] and refs. therein.) This, in combination with the hygroscopic nature of many ionic liquids, is at the core of the disagreements in the literature. In view of these results, the sample of $[C_6mim][NTf_2]$ used by the participants in this IUPAC project was carefully synthesized, characterized, and handled by all research groups, with particular care with regard to water contamination. Most researchers included coulometric Karl Fischer titrations before and after their measurements to demonstrate the absence of significant amounts of water. Full details of the synthesis and analysis have been published [4]. The sample was demonstrated to have a mole fraction purity greater than 0.995 by a variety of methods and a water mass fraction less than 0.000 01 [4]. A fractional melting study with adiabatic calorimetry [5] showed the mole fraction purity of the sample to be 0.9976.

DATA CAPTURE AND CRITICAL EVALUATION PROCEDURES

All of the available experimental property data for $[C_6mim][NTf_2]$ were compiled at the NIST Thermodynamics Research Center (TRC) Data Entry Facility using guided data capture (GDC) software previously described [6]. All values were checked for typographical errors and obvious inconsistencies before loading into the NIST/TRC SOURCE Data Archival System [7,8]. Recommended values were derived based on weighted averaging for single-valued properties and weighted fitting of appropriate equations for properties involving independent variables. Weights were based upon estimated combined expanded uncertainties for the experimental values. All averaging and curve fitting procedures were done with the aid of the NIST ThermoData Engine [9,10] data expert system software.

The expressions of uncertainty in this paper conform to the *Guide to the Expression of Uncertainty in Measurement*, ISO (International Organization for Standardization), October, 1993 [11]. Reference [1] is commonly referred to by its abbreviation—the GUM. The recommendations have been summarized in *Guidelines for the Evaluation and Expression of Uncertainty in NIST Measurement Results* [12], which is available via free download from the Internet (<http://physics.nist.gov/cuu/>; accessed 20 January 2009). Recently, the recommendations of the GUM were summarized with particular application to the reporting of experimental thermodynamic property data [13].

All uncertainties given in this article are expressed as the combined expanded uncertainty with coverage factor $k = 2$, corresponding to a confidence level of approximately 95 %.

PURE COMPOUND PROPERTIES

Phase behavior in the condensed state

Heat capacities and phase transformations in the condensed state for the IUPAC sample of $[C_6mim][NTf_2]$ were studied with adiabatic calorimetry [5,14] and differential scanning calorimetry (DSC) [15]. The same general phase behavior was observed by all researchers. Upon initial cooling the sample of $[C_6mim][NTf_2]$ did not crystallize, but formed a glass with a glass-transition temperature within several kelvins of T = 185 K. Crystallization was initiated when the sample was reheated above the glass-transition temperature, however, the crystals that formed initially were metastable. The normal melting temperature T_m of these metastable crystals was observed to be near T = 266 K by Archer [15] and Shimizu et al. [14]. Conversion from the metastable to stable crystals ($T_m \approx 272.1$ K) occurred spontaneously, but slowly. Indeed, several early studies [16,17] reported the lower value as T_m for the stable crystals.

Careful DSC by Archer revealed the presence of a crystal-to-crystal transformation in the metastable crystal form of $[C_6mim][NTf_2]$. The enthalpy of this transition (centered near T = 231 K) was shown to decrease on repeated scans through the region between T = 203 K and T = 258 K, as the sample converted to the stable form at the higher temperatures. The enthalpy of the transition was found to be essentially invariant, if the upper limit of the cycled range was less than T = 253 K. The presence of the crystal-to-crystal transition in the metastable crystal form can also be seen in the adiabatic calorimetric results of Blokhin et al. [5], as discussed later with the heat capacity evaluations.

In studies with adiabatic calorimetry, Shimizu et al. [14] annealed the sample for three days near T = 215 K and did not report evidence for the metastable phase. Blokhin et al. [5] always annealed their sample more than 20 K above this temperature and encountered problems with irreproducible results for T > 220 K in the crystal phase. Because of the lack of evidence for the presence of the metastable crystal phase, plus the fact that they reported the highest enthalpy of fusion for the ionic liquid (indicating the most complete conversion from the liquid to the crystal form), the results by Shimizu et al. [14] are considered the most reliable for the stable crystal phase and for the properties of the crystal-to-liquid transition.

Triple-point temperature

Experimental values reported for the triple-point temperature T_{tp} are listed in Table 1 together with values for the normal melting temperature. Results of measurements for samples other than the IUPAC sample are included in the table. Uncertainties for the experimental values are those provided by the authors. Often, these are not the combined expanded uncertainty, so direct comparisons or statistical weightings based on these values are not possible. (Issues related to the reporting of uncertainties in the literature were discussed recently [18].) The recommended value for T_{tp} is that measured by Shimizu et al. [14], with the estimated uncertainty based on the experimental method, plus typical uncertainties associated with thermometer calibrations and temperature gradients in similar calorimeters.

Table 1 Triple-point temperature, enthalpy of fusion, and glass-transition temperature for $[C_6mim][NTf_2]$.

Data source	Method[a]	T_{tp}/K	$\Delta^l_{cr} H$/kJ mol^{-1}	T_g/K	Sample
Shimizu et al. [14]	AC	272.13[b]	28.34[b]	183	IUPAC
Blokhin et al. [4]	AC	(272.03 ± 0.01)[c]	(28.09 ± 0.08)[c]	184.3	IUPAC
Archer [15]	DSC	(272.11 ± 0.29)[d]	(27.83 ± 0.35)[d]	190	IUPAC
Tokuda et al. [17]	DSC	267.1[b,e,f]	4.6[b]	192	non-IUPAC
Crosthwaite et al. [16]	DSC	266[f]		189	non-IUPAC
Recommendations		(272.13 ± 0.05)[g]	(28.34 ± 0.08)[g]	none	

[a]AC = adiabatic calorimetry, DSC = differential scanning calorimetry.
[b]The uncertainty was not estimated by the authors.
[c]The uncertainty listed here is the repeatability provided by the authors.
[d]The combined expanded uncertainty ($k = 2$) estimated by the author.
[e]This value was reported in the original source as –6 °C.
[f]This value was demonstrated by Archer [15] and Shimizu et al. [14] to be the melting temperature of a metastable crystal form.
[g]The estimated combined expanded uncertainty with a 95 % level of confidence.

Enthalpy of fusion

Experimental values reported for the enthalpy of fusion $\Delta^l_{cr} H$ are also listed in Table 1 with uncertainties provided by the authors. The very low value of $\Delta^l_{cr} H$ from the work of Tokuda et al. [17] is for the metastable crystal form. The recommended value for the enthalpy of fusion is that measured by Shimizu et al. [14], with the uncertainty estimation based on the experimental method. Values determined by Archer [15] and Blokhin et al. [5] are slightly lower. Although the listed values for the enthalpy of fusion determined with adiabatic calorimetry by Shimizu et al. [14] and Blokhin et al. [5] differ by approximately 0.9 %, this difference probably can be attributed to less complete annealing of the sample by Blokhin et al. [5].

Glass-transition temperature

The various reported glass-transition temperatures are listed in Table 1. No recommendation is given for this quantity because it is dependent on the thermal history of the sample, and is not a thermodynamic property.

Heat capacities for the crystal state

Blokhin et al. [5] reported results for an "alpha", "beta", and "gamma" crystal form that, in retrospect, are the results of different degrees of annealing of the stable crystal form. Heat capacities reported by Blokhin et al. [5] for the "beta" and "gamma" crystals are lower than those for the "alpha" form as the triple-point temperature is approached, which can be indicative of slow annealing of the sample (i.e., conversion to the stable crystal form). This implies that the results for the "alpha" crystal reported by Blokhin et al. [14] should most nearly approximate those of the stable crystal form. As noted earlier, heat capacity values reported by Shimizu et al. [5] appear to be the most reliable for the crystal phase, however, they did not make an extensive study of the annealing procedures, so at this time, these measurements cannot be considered definitive.

A comparison of the adiabatic calorimetric results of Blokhin et al. [5] and Shimizu et al. [14] is shown in Fig. 2. The agreement between these studies is fair for temperatures $T < 200$ K and in the liquid phase ($T > 272.1$ K) with differences, generally, within 0.4 %, which is the relative uncertainty claimed by Blokhin et al. [5] for their results in the temperature range $20 < (T/\text{K}) < 370$. Shimizu et al.

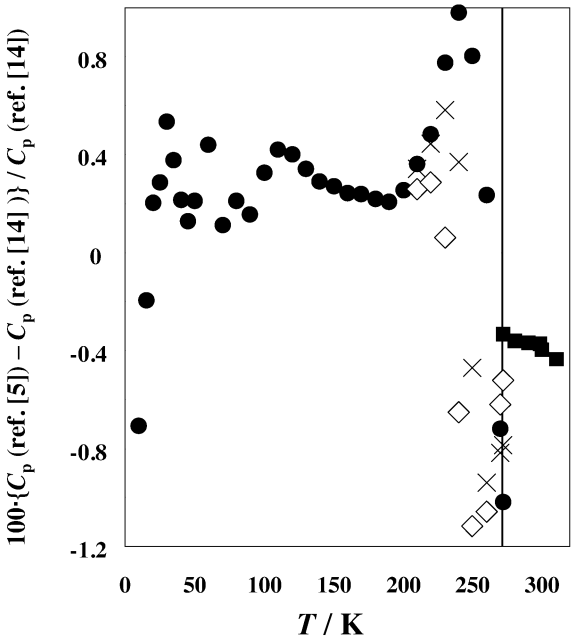

Fig. 2 Difference plot for condensed-phase heat capacities C_p (p = 0.1 MPa) measured by Blokhin et al. [5] from those by Shimizu et al. [14]. The vertical line indicates the triple-point temperature (T_{tp} = 272.13 K). The symbols represent results for various forms of the ionic liquid reported by Blokhin et al. [5]: ●, "alpha" crystals; ×, "beta" crystals; ◇, "gamma" crystals; ■, liquid. See text for crystal form descriptions. The IUPAC sample was used in both studies.

[14] reported a detailed uncertainty budget for one heat capacity value in the liquid at T = 298.15 K, which yielded a combined expanded uncertainty (with k = 2) of slightly less than 0.1 %.

The general features of the observed differences for the crystal phase can be understood with the aid of the DSC study by Archer [15]. With DSC, measurements can be made in rapid succession with small sample sizes. This allows detection of thermal events that cannot be observed with traditional adiabatic calorimetry because the rate of measurements with DSC is several orders of magnitude faster than with adiabatic calorimetry. The excess heat capacity above T = 200 K in the results reported by Blokhin et al. [5] (Fig. 2) probably arises from the presence of the crystal-to-crystal phase transition in the metastable crystal form of $[C_6mim][NTf_2]$ shown by Archer [15]. The low heat capacities by Blokhin et al. [5] between T = 230 K and T_{tp} might be attributed to spontaneous warming of the sample caused by the conversion from the metastable to stable forms. Results by Shimizu et al. [14] showed no evidence of excess heat capacity or phase conversion after annealing of the sample near T = 215 K. Blokhin et al. [5] did not anneal their sample at temperatures lower than $T \approx$ 237 K, which might underlie some of the differences observed for the crystal state.

Although the results by Shimizu et al. [14] are considered the most reliable for the crystal state, recommendations for heat capacities of the crystal state cannot be made at this time because of the complex solid-state behavior. Further calorimetric and structural studies are justified.

Heat capacities for the liquid state (near pressure p = 0.1 MPa)

In addition to the adiabatic calorimetric results reported by Blokhin et al. [5] and Shimizu et al. [14], Archer [15] reported heat capacities for the IUPAC sample in the liquid phase measured with DSC. The recommended values are the result of a weighted least-squares fit of a polynomial to these values.

$$C_p/(\text{J K}^{-1}\ \text{mol}^{-1}) = -1580.27 + 41.9143\cdot(T/\text{K}) - 0.325\ 398\cdot(T/\text{K})^2 + 1.247\ 75\cdot10^{-3}\cdot(T/\text{K})^3 - 2.338\ 75\cdot10^{-6}\cdot(T/\text{K})^4 + 1.719\ 84\cdot10^{-9}\cdot(T/\text{K})^5 \quad (1)$$

The equation is valid from near the glass-transition temperature (T = 190 K) to the high-temperature limit of the values reported by Blokhin et al. [5] (T = 370 K). The combined expanded uncertainties for the heat capacities of the liquid are 0.6 % at T = 190 K, decrease linearly with temperature to 0.2 % at T_{tp}, and increase linearly to 0.5 % at T = 370 K.

A deviation plot for all measurements of heat capacity for the liquid phase is shown in Fig. 3. Deviations for studies done on non-IUPAC samples of $[C_6mim][NTf_2]$ by Crosthwaite et al. [16], Diedrichs and Gmehling [19], and Ge et al. [20] are included in Fig. 3. Deviations of the results obtained with DSC [15,16,19,20] are surprisingly large. Uncertainties for heat capacities obtained with DSC are typically near 2 % and can be even less. The origin of these deviations is unknown.

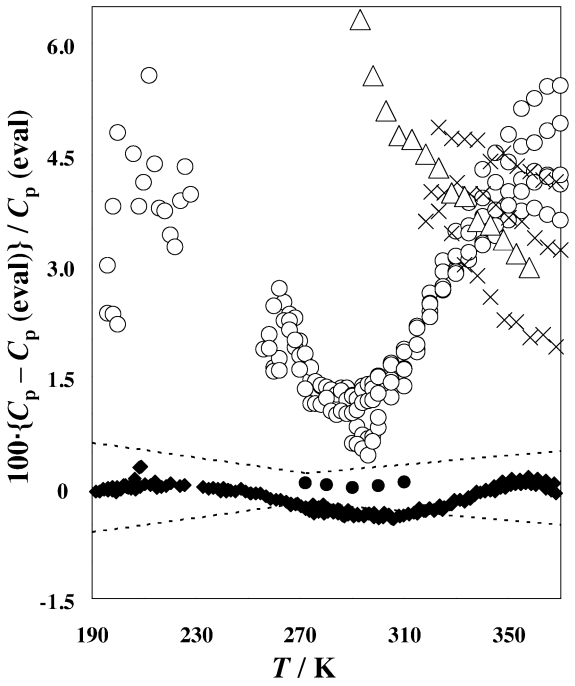

Fig. 3 Deviation plot for experimental heat capacities C_p (p = 0.1 MPa) for the liquid phase of $[C_6mim][NTf_2]$ relative to the critically evaluated values C_p(eval) calculated with eq. 1. ●, Shimizu, et al. [14]; ◆, Blokhin et al. [5]; ○, Archer [15]; ×, Diedrichs and Gmehling [19] (non-IUPAC sample); △, Ge et al. [20] (non-IUPAC sample). Values reported by Crosthwaite et al. [16] for T = 298.15 K and T = 323.1 for a non-IUPAC sample are approximately 7 % low and are not shown. The dashed lines represent the combined expanded uncertainties for C_p(eval).

Density of the liquid (near pressure p = 0.1 MPa)

Densities of the IUPAC sample for the liquid state near pressure p = 0.1 MPa were measured by Lachwa et al. [21] {293 < (T/K) < 303}, Kandil et al. [22] {298 < (T/K) < 423}, Widegren and Magee [4] {258 < (T/K) < 373}, Esperanca et al. [23] {293 < (T/K) < 338}, Seddon and Driver [3,24] {293 < (T/K) < 363}, and Domanska and Marciniak [25] (T = 298 K). Density values determined with other samples of $[C_6mim][NTf_2]$ were reported by Fitchett et al. [26] (T = 295 K), Aki et al. [27] {298 < (T/K) < 333},

Gomes de Azevedo et al. [28] {298 < (*T*/K) < 333}, Kato and Gmehling [29] {293 < (*T*/K) < 358}, Lopes et al. [30] {298 < (*T*/K) < 333}, Tokuda et al. [17] {288 < (*T*/K) < 323}, Kumelan et al. [31] {290 < (*T*/K) < 307}, Tokuda et al. [32] {288 < (*T*/K) < 313}, and Muhammad et al. [33] {298 < (*T*/K) < 358}.

Recommended values were determined with a weighted least-squares fit to all values determined with the IUPAC sample except those by Lachwa et al. [21]. (Lachwa et al. were most interested in determination of excess volumes and liquid–liquid equilibria (LLE) with alcohols, and their ionic liquid sample was subject to varying degrees of degassing and drying.) The recommended values are expressed by the following equation for the temperature range 258 < (*T*/K) < 373. The combined expanded uncertainty (with $k = 2$) is estimated to be 0.1 % for the entire temperature range.

$$\rho/(\text{kg m}^{-3}) = 1640.95 - 0.9012 \cdot (T/\text{K}) \quad (2)$$

The density ρ at $T = 298.15$ K calculated with this equation is (1372.21 ± 1.37) kg m^{-3}. This value is provided here as a convenient check for proper implementation of the equation in a computer program by the reader. Analogous values are given for all critically evaluated properties represented with equations.

Deviations for all of the studies involving the IUPAC sample are shown in Fig. 4, and those involving samples other than the IUPAC sample are shown in Fig. 5. In Fig. 4, the results of Lachwa et al. [21] are generally quite low, and in Fig. 5, it is seen that nearly all deviations from the recommended values are negative. Both of these observations are consistent with the samples not being completely dried, as discussed by Widegren and Magee [4].

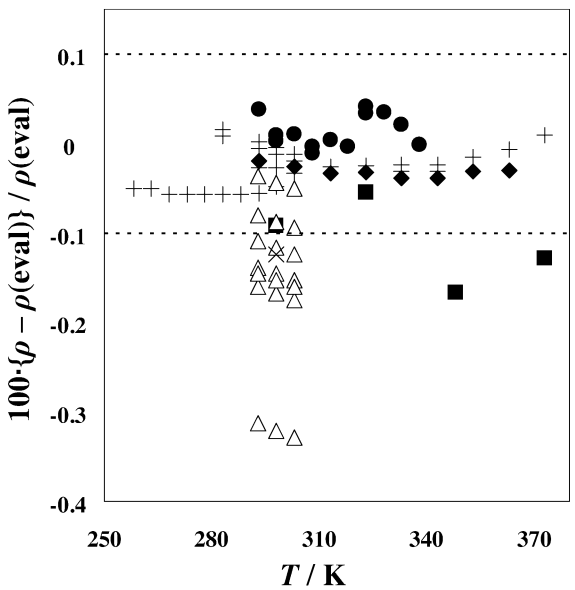

Fig. 4 Deviation plot for experimental densities ρ for the IUPAC sample of [C_6mim][NTf_2] near pressure $p = 0.1$ MPa from the critically evaluated values ρ(eval) calculated with eq. 2. ■, Kandil et al. [22]; +, Widegren and Magee [4]; ●, Esperanca et al. [23]; ◆, Seddon and Driver [3,24]; ×, Domanska and Marciniak [25]; △, Lachwa et al. [21]. Water and air content was not controlled by Lachwa et al. [21]. The dashed lines represent the combined expanded uncertainties for ρ(eval).

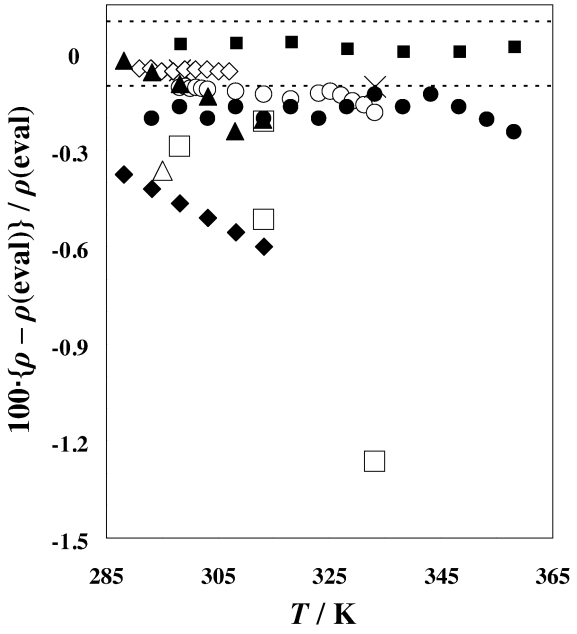

Fig. 5 Deviation plot for experimental densities ρ from the critically evaluated values ρ(eval) for non-IUPAC samples of $[C_6mim][NTf_2]$ near pressure p = 0.1 MPa. □, Aki et al. [27]; ○, Gomes de Azevedo et al. [28]; △, Fitchett et al. [26]; ●, Kato and Gmehling [29]; ×, Lopes et al. [30]; ◆, Tokuda et al. [17]; ◇, Kumelan et al. [31]; ▲, Tokuda et al. [32], ■, Muhammad et al. [33]. Values of ρ(eval) were calculated with eq. 2. The dashed lines represent the combined expanded uncertainties for ρ(eval).

Density of the liquid at high pressures

Densities of the IUPAC sample of $[C_6mim][NTf_2]$ for the liquid state at high pressures were determined by Kandil et al. [22] {298 < (T/K) < 423, 0.1 < p/MPa < 40} and Esperanca et al. [23] {293 < (T/K) < 338, 0.1 < p/MPa < 65}. Earlier, measurements on an independent sample of $[C_6mim][NTf_2]$ were published by Gomes de Azevedo et al. [28] {298 < (T/K) < 333, 0.1 < p/MPa < 60}. References [23] and [28] represent results from the same laboratory. The earlier measurements [28] were made on a sample that contained as much as 0.0075 mass fraction water, which has been shown to result in densities that are low by approximately 0.3 % [4].

Recommended values were determined with a weighted least-squares fit of the Tait equation to all values determined with the IUPAC sample. The form of the Tait equation used is expressed as follows:

$$\rho = \rho^{\circ}/[1 - c\cdot\ln\{(b + p/\text{kPa})/(b + 101.3)\}] \quad (3)$$

where ρ° is the density at reference pressure 101.3 kPa (calculated with eq. 2), $b = \Sigma\, B_i\cdot\tau^i$ (with summation over i = 0 to 3), $c = \Sigma\, C_i\cdot\tau^i$ (with summation over i = 0 to 2) and, $\tau = (T/\text{K} - 293.15)/100$. The fitted parameters are 175 140, –516 809, 817 749, and –186 296 for B_0 to B_3, respectively, and 0.0927 279, –0.215 34, and 0.336 983 for C_0 to C_2. The densities ρ at T = 298.15 K for the pressures (20, 40, and 60) MPa calculated with this equation are (1386.5 ± 2.0) kg m^{-3}, (1399.5 ± 2.6) kg m^{-3}, and (1411.3 ± 3.2) kg m^{-3}, respectively.

Deviations for the high-pressure studies as a function of temperature and pressure are shown in Figs. 6 and 7, respectively. The early study by Gomes de Azevedo et al. [28] on the non-IUPAC sample are lower than the recommended values, as expected because of the presence of small amounts of water. Kandil et al. [22] estimated the combined expanded uncertainties (k = 2) for their values to be

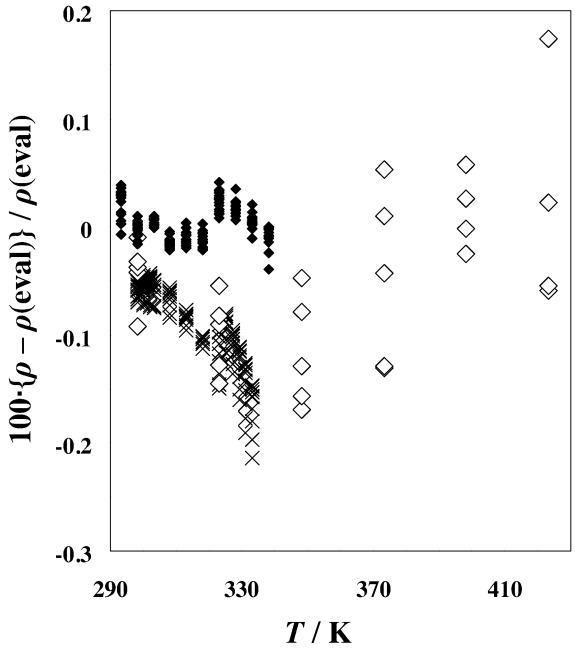

Fig. 6 Deviation plot for experimental densities ρ at elevated pressures from the critically evaluated values ρ(eval) calculated with eq. 3 for $[C_6mim][NTf_2]$ and shown as a function of temperature. ◇, Kandil et al. [22]; ◆, Esperanca et al. [23]; ×, Gomes de Azevedo et al. [28] (non-IUPAC sample).

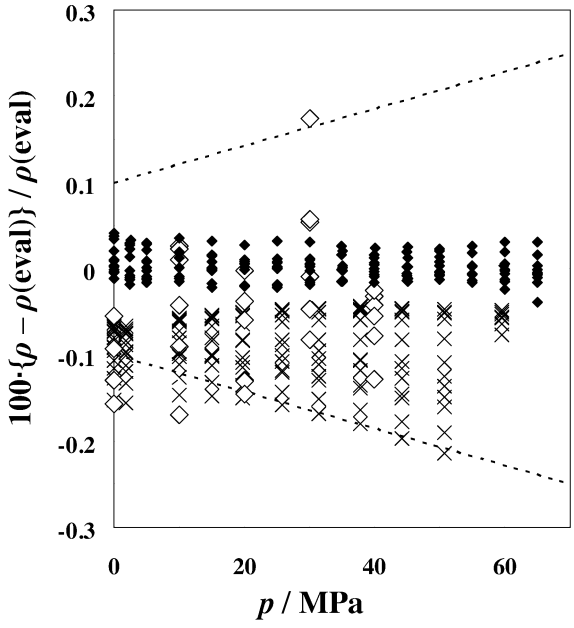

Fig. 7 Deviation plot for experimental densities ρ at elevated pressures from the critically evaluated values ρ(eval) calculated with eq. 3 for $[C_6mim][NTf_2]$, shown as a function of pressure. ◇, Kandil et al. [22]; ◆, Esperanca et al. [23]; ×, Gomes de Azevedo et al. [28] (non-IUPAC sample). The dashed lines represent the combined expanded uncertainties for ρ(eval).

0.3 %. Esperanca et al. [23] estimated their combined uncertainties to be 1.5 kg m^3 without indication of the level of confidence. The combined expanded uncertainties ($k = 2$) of the recommended values are 0.1 % at $p = 0.1$ MPa and increase linearly to 0.25 % at $p = 70$ MPa for all temperatures.

Vapor pressure

The vapor pressure of the IUPAC sample of $[C_6mim][NTf_2]$ was measured by Zaitsau et al. [34] with Knudsen effusion methods between the temperatures $T = 446$ K and $T = 494$ K. The observed pressures p ranged from $p = 0.007$ Pa to $p = 0.17$ Pa. No recommended values are given here, as this was the only set of such measurements performed. It is difficult to assess uncertainties for these measurements because of the very low pressures involved and the lack of related thermodynamic properties for demonstration of thermodynamic consistency. Uncertainty estimates were not provided by the authors.

Viscosity of the liquid (near pressure $p = 0.1$ MPa)

Viscosities of the IUPAC sample of $[C_6mim][NTf_2]$ were measured by Kandil et al. [22] {298 < (T/K) < 423}, Widegren and Magee [4] {258 < (T/K) < 373}, Santos et al. [35] {298 < (T/K) < 343}, and Seddon and Driver [24] {298 < (T/K) < 368}. Viscosity values determined with non-IUPAC samples were reported by Fitchett et al. [26] ($T = 295$ K), Crosthwaite et al. [16] {283 < (T/K) < 343}, Tokuda et al. [17] {283 < (T/K) < 353}, Tokuda et al. [32] {283 < (T/K) < 353}, Ahosseini and Scurto [36] {298 < (T/K) < 343}, and Muhammad et al. [33] {288 < (T/K) < 328}.

Recommended values were determined with a weighted least-squares fit of eq. 4 to all values determined with the IUPAC sample.

$$\ln(\eta/\eta^\circ) = -13.941 + 6721.88/(T/\mathrm{K}) - 2.245\,84\cdot10^6/(T/\mathrm{K})^2 + 3.708\,41\cdot10^8/(T/\mathrm{K})^3 \quad (4)$$

where $\eta^\circ = 1$ Pa s. The temperature range of validity is 258 < (T/K) < 433. The viscosity η at $T = 298.15$ K calculated with this equation is (0.0694 ± 0.0014) Pa s. The values reported by Seddon and Driver [24] are anomalously high and were not included in the fit. Deviations for all of the viscosity studies are shown in Fig. 8. The combined expanded uncertainties for the viscosity values are 2 % for values from $T = 298.15$ K to T = 370 K, and increase linearly to 5 % at the limits of the validity range.

In addition to values near $p = 0.1$ MPa, Kandil et al. [22] reported viscosities for pressures up to $p = 50$ MPa over the entire temperature range. As this was the only set of such measurements made, no recommendations are given here. The combined expanded uncertainty ($k = 2$) given by the authors was 2 %. Ahosseini and Scurto [36] also reported viscosities at high pressures (to 124 MPa) for a non-IUPAC sample with an estimated uncertainty (undefined) near 3 %. These values are consistent with the recommended values near 0.1 MPa given in this paper and with the high-pressure results of Kandil et al. [22].

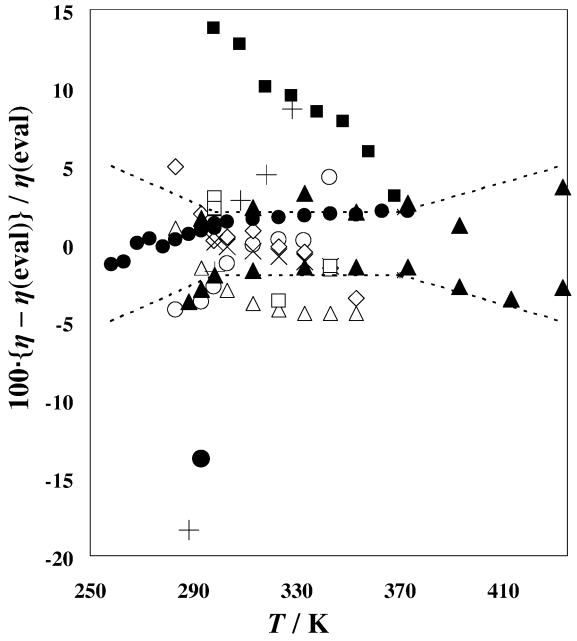

Fig. 8 Deviation plot for experimental viscosities η from the critically evaluated values η(eval) calculated with eq. 4 for [C_6mim][NTf_2] near pressure p = 0.1 MPa. The IUPAC sample was studied by: ▲, Kandil et al. [22]; ×, Santos et al. [35]; ●, Widegren and Magee [4]; ■, Seddon and Driver [24]. Non-IUPAC samples were studied by: ●, Fitchett et al. [26]; ○, Crosthwaite et al. [16]; △, Tokuda et al. [17]; ◇, Tokuda et al. [32]; □, Ahosseini and Scurto [36]; +, Mohammad et al. [33]. The dashed lines represent the combined expanded uncertainties for η(eval).

Electrolytic conductivity (near pressure p = 0.1 MPa)

The electrolytic conductivity of the IUPAC sample of [C_6mim][NTf_2] was measured by Kandil et al. [22] {278 < (T/K) < 323}, Widegren et al. [37] {288 < (T/K) < 323}, and Widegren and Magee [4] {288 < (T/K) < 323}. Expanded combined uncertainties (k = 2) were estimated to be 2 % by all researchers using the IUPAC sample. Values determined with non-IUPAC samples were reported by Tokuda et al. [17] {263 < (T/K) < 373} and Tokuda et al. [32] {263 < (T/K) < 373}.

Recommended values were determined with a weighted least-squares fit of eq. 5 to all values determined with the IUPAC sample. Deviations for all of the measured electrolytic conductivities are shown in Fig. 9. Electrolytic conductivity κ as a function of temperature for the IUPAC sample of [C_6mim][NTf_2] is represented by the following polynomial:

$$\kappa/(\mathrm{S\ m^{-1}}) = 0.2903 + 0.01969\cdot(T/\mathrm{K}) - 1.666\cdot10^{-4}\cdot(T/\mathrm{K})^2 + 3.345\cdot10^{-7}\cdot(T/\mathrm{K})^3 \quad (5)$$

The range of validity is 278 < (T/K) < 323. The estimated combined expanded uncertainties (k = 2) for the electrolytic conductivity values are 2 %. The electrolytic conductivity κ at T = 298.15 K calculated with this equation is (0.2167 ± 0.0043) S m^{-1}. Tokuda et al. [17,32] also reported values at temperatures outside of the range of validity for eq. 5, and these are not shown in Fig. 9.

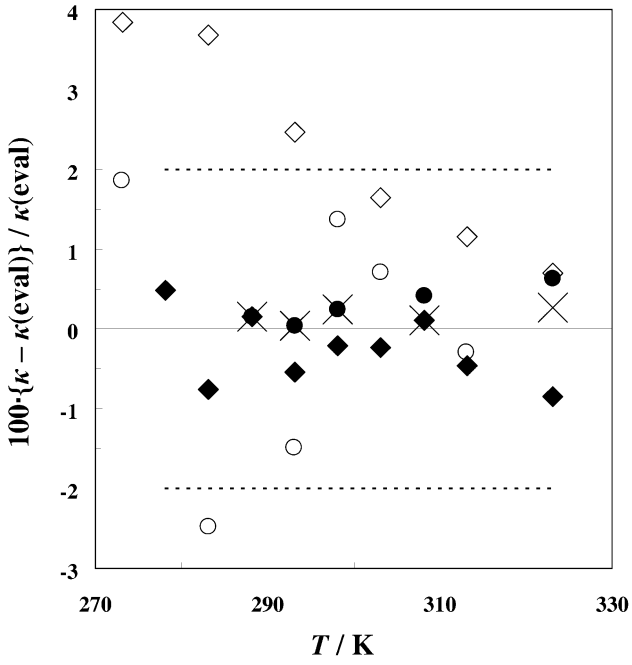

Fig. 9 Deviation plot for experimental electrolytic conductivities κ from the critically evaluated values κ(eval) calculated with eq. 5 for [C_6mim][NTf_2] near pressure p = 0.1 MPa. The IUPAC sample was studied by: ×, Widegren et al. [37]; ◆, Kandil et al. [22]; ●, Widegren and Magee [4]. Non-IUPAC samples were studied by: ◇, Tokuda et al. [17]; ○, Tokuda et al. [32]. The dashed lines represent the combined expanded uncertainties for κ(eval).

Speed of sound (near pressure p = 0.1 MPa)

Widegren and Magee [4] measured the speed of sound in the IUPAC sample of [C_6mim][NTf_2] for the temperature range 283 < (T/K) < 343. The combined expanded uncertainty (k = 2) estimated by the authors was 1.7 m s^{-1}. This uncertainty is recommended here. The speeds of sound can be represented with the following equation:

$$(u/\text{m s}^{-1}) = 2139.4 - 3.8284\cdot(T/\text{K}) + 2.5772\cdot10^{-3}\cdot(T/\text{K})^2 \quad (6)$$

The speed of sound u at T = 298.15 K calculated with this equation is (1227.1 ± 1.7) m s^{-1}. Frez et al. [38] determined the speed of sound for [C_6mim][NTf_2] at T = 298.15 K with a transient grating method. Their value is 6 m s^{-1} lower (i.e., 0.5 % lower) than that of Widegren and Magee [4].

Other property measurements (near pressure p = 0.1 MPa)

Hunger et al. [39] measured the relative permittivity for the IUPAC sample of [C_6mim][NTf_2] for the temperature range 278 < (T/K) < 338. This was the only set of such measurements performed, and no recommended values are given here. The surface tension of [C_6mim][NTf_2] was measured by Kilaru et al. [40] {297 < (T/K) < 346}, Carvalho et al. [41] {293 < (T/K) < 343}, and Muhammad et al. [33] {298 < (T/K) < 338}, all with non-IUPAC samples. The values reported by Kilaru et al. [40] are approximately 12 % higher than values from the other research groups, as well as a single unpublished value provided by Domanska and Marciniak [42] (T = 298.15 K) for the IUPAC sample. The thermal conductivity of [C_6mim][NTf_2] was measured by Ge et al. [43] for a non-IUPAC sample between the temperatures T = 293 K and T = 353 K. No recommended values are given here for these properties.

Effect of water on the properties of $[C_6mim][NTf_2]$

The effect of water on the properties of the $[C_6mim][NTf_2]$ was studied by Widegren and Magee [4] (densities, viscosities, speeds of sound, and electrolytic conductivities) and Widegren et al. [37] (electrolytic conductivities). Figures 10–13 show the variation of these properties with water content, as reported by Widegren and Magee [4]. In these figures, the properties are shown as a function of water content expressed in mole fraction of H_2O. The mole fraction solubility of water x in $[C_6mim][NTf_2]$

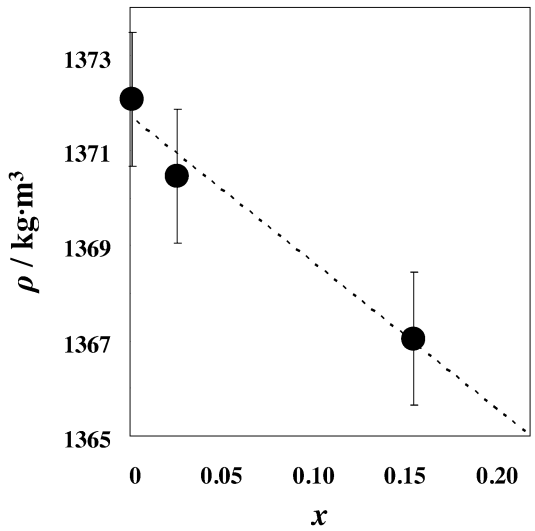

Fig. 10. Density of $[C_6mim][NTf_2]$ as a function of water content expressed as water mole fraction x, as determined by Widegren and Magee [4] for temperature $T = 298.15$ K and pressure $p \approx 0.1$ MPa. The dashed line is a guide for the eye. The error bars represent the combined expanded uncertainties ($k = 2$) estimated by the authors [4].

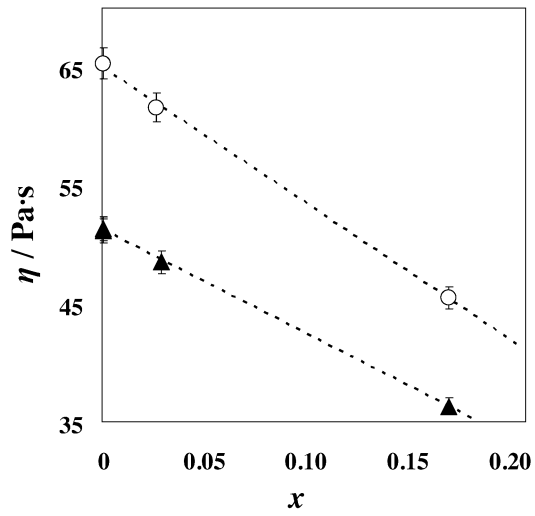

Fig. 11 Viscosity of $[C_6mim][NTf_2]$ as a function of water content expressed as water mole fraction x, as determined by Widegren and Magee [4] at pressure $p \approx 0.1$ MPa. ○, temperature $T = 293.15$ K; ▲, $T = 298.15$ K. The dashed lines are guides for the eye. The error bars represent the combined expanded uncertainties ($k = 2$) estimated by the authors [4].

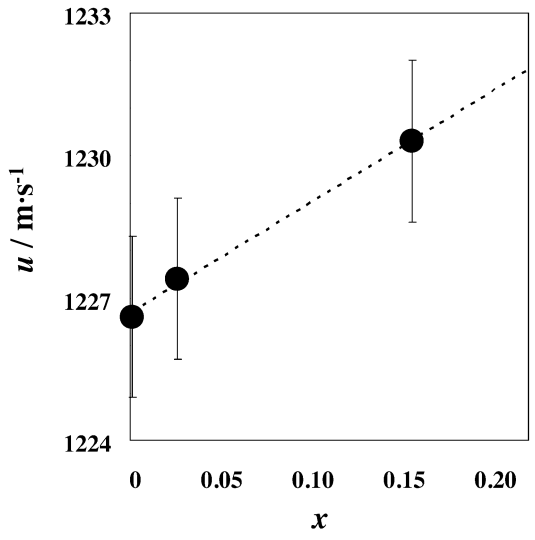

Fig. 12 Speed of sound in $[C_6mim][NTf_2]$ as a function of water content expressed as water mole fraction x, as determined by Widegren and Magee [4]. ●, temperature T = 298.15 K and pressure $p \approx 0.1$ MPa. The dashed line is a guide for the eye. The error bars represent the combined expanded uncertainties ($k = 2$) estimated by the authors [4].

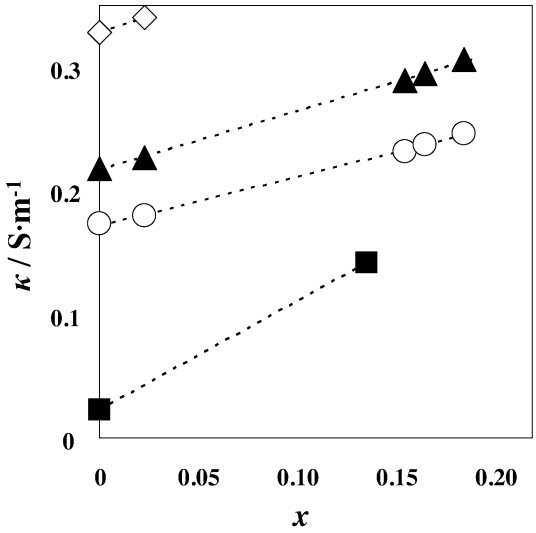

Fig. 13 Electrolytic conductivity of $[C_6mim][NTf_2]$ as a function of water content expressed as water mole fraction x, as determined by Widegren and Magee [4] at pressure $p \approx 0.1$ MPa. ■, temperature T = 288.15 K; ○, T = 293.15 K; ▲, T = 298.15 K; ◇, T = 303.15 K. The dashed lines are guides for the eye. The combined expanded uncertainties ($k = 2$) estimated by the authors [4] is 2 %.

is near $x = 0.22$, as discussed later. The four figures were drawn so that the upper extreme of the horizontal axis corresponds approximately to the water saturation limit.

Water contents for ionic liquids are often expressed in mass fraction of water. Because of the large difference in molecular mass between the two components, this can give a misleading impression concerning the amount of water present. For example, in the case of $[C_6mim][NTf_2]$, mass fraction water

$w = 0.01$ corresponds to mole fraction $x = 0.20$. In view of this, plus the hygroscopic nature of ionic liquids, it is apparent that many of the inconsistencies between properties of ionic liquids reported in the literature by different research groups can be traced to inadequate control of water exposure. A review of the deviation plots for the various properties discussed above shows that most large deviations of results for non-IUPAC samples from the recommended values can be accounted for, if the presence of water is assumed.

MIXTURE PROPERTIES (VAPOR–LIQUID EQUILIBRIA)

Vapor–liquid equilibrium with CO_2 ("gas solubility")

The solubility of CO_2 in the IUPAC sample of $[C_6mim][NTf_2]$ was measured by Kumelan et al. [31], Costa Gomes [44], Muldoon et al. [45], Shiflett and Yokozeki [46], and Peters and coworkers [47]. In addition, several research groups reported CO_2 solubilities for non-IUPAC samples; Aki et al. [27], Kim et al. [48], Kim et al. [49], and Shin et al. [50]. The temperature and pressure ranges for each study are shown in Fig. 14.

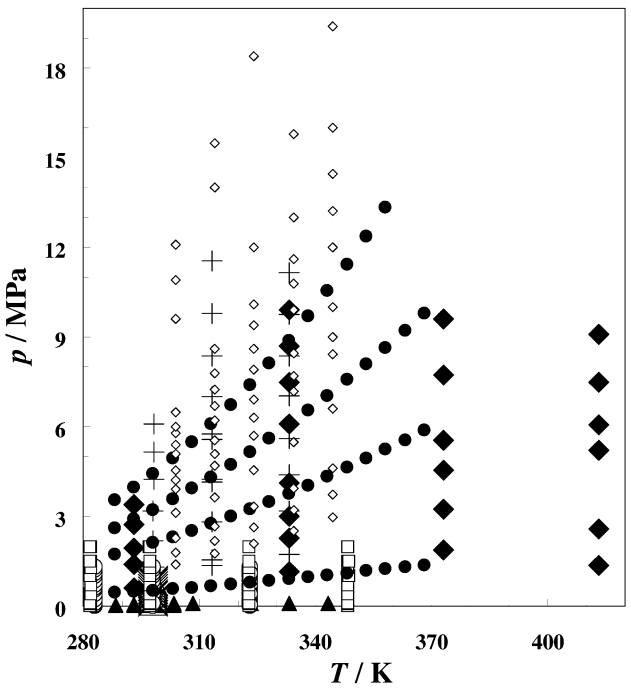

Fig. 14 Temperature and pressure ranges for solubility-pressure (or "gas solubility") studies for the chemical system (carbon dioxide + $[C_6mim][NTf_2]$). The IUPAC sample of $[C_6mim][NTf_2]$ was used by: ◆, Kumelan et al. [31]; ▲, Costa Gomes [44]; ○, Muldoon et al. [45]; □, Shiflett and Yokozeki [46]; ●, Peters and coworkers [47]. Non-IUPAC samples were used by: +, Aki et al. [27]; △, Kim et al. [48]; ×, Kim et al. [49]; ◇, Shin et al. [50].

The solubility pressures for the studies with the IUPAC sample were modeled with a method similar to that described by Kumelan et al. [31] involving the "extended" Henry's law. The model allows comparisons between the diverse data sets and convenient representation of recommended values. The recommended values of solubility pressures p are expressed with the following equations:

$$\left(p/\mathrm{kPa}\right) = k_{\mathrm{H,CO_2}} \cdot m_1 \cdot \exp\left\{\sum_{i=1}^{2}\sum_{j=0}^{1} a_{ij} \cdot x_1^i \cdot (T/K)^j\right\}, \text{where} \tag{7}$$

$$k_{\mathrm{H,CO_2}} = 30.965 - 2351.6/(T/\mathrm{K}) - 2.6365 \cdot \ln(T/\mathrm{K}), \tag{8}$$

and $k_{\mathrm{H,CO_2}}$ is the Henry's law constant of CO_2(g) in [C_6mim][NTf_2] on the molality scale, and m_1 and x_1 are the molality and mole fraction of CO_2 in the liquid phase, respectively. The parameters of eq. 8 were determined though fitting of $k_{\mathrm{H,CO_2}}$ values derived with extrapolations of the experimental values from higher pressures. The elements of the a matrix are: $a_{1,0}$ = 0.636 666, $a_{2,0}$ = –4.289 230, $a_{1,1}$ = –0.001 897, and $a_{2,1}$ = 0.011 980. Deviation plots for all of the VLE studies with carbon dioxide are shown in Fig. 15 (as percent deviations) and Fig. 16 (as absolute deviations). For mole fractions of carbon dioxide $x_{\mathrm{CO_2}} \geq 0.1$, the combined expanded uncertainty (k = 2) for the solubility pressure is estimated to be 10 % of the pressure p for $x_{\mathrm{CO_2}}$ = 0.1 and decreases to 5 % for $x_{\mathrm{CO_2}}$ = 0.7. The upper temperature and pressure limits of the recommended values are T = 413 K and p = 13 MPa. For $x_{\mathrm{CO_2}} < 0.1$, the combined expanded uncertainty (k = 2) is estimated to be the greater of 0.1·p and 40 kPa for $x_{\mathrm{CO_2}}$ = 0.1, and falls to the greater of 0.1·p and 5 kPa, as $x_{\mathrm{CO_2}} \rightarrow 0$. Evaluated solubility pressures for some specific conditions are listed in Table 2.

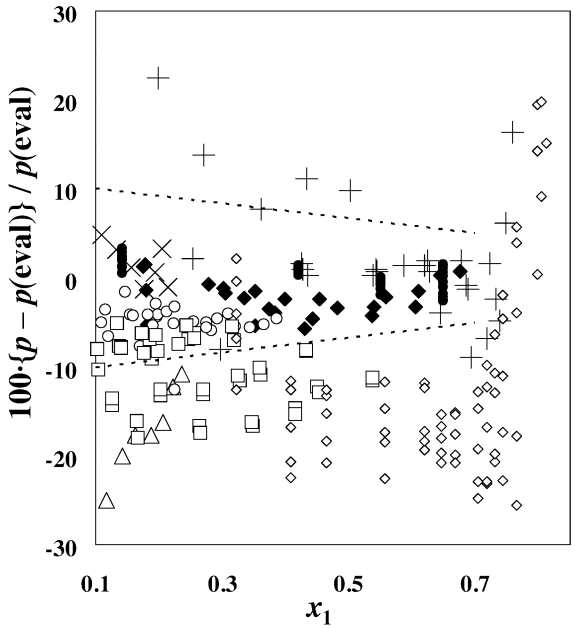

Fig. 15 Deviation plot (percent deviations) for experimental solubility pressures p from the critically evaluated values p(eval) calculated with eq. 7 for the system {carbon dioxide (1) + [C_6mim][NTf_2] (2)}. The IUPAC sample of [C_6mim][NTf_2] was used by: ◆, Kumelan et al. [31]; ▲, Costa Gomes [44]; ○, Muldoon et al. [45]; □, Shiflett and Yokozeki [46]; ●, Peters and coworkers [47]. Non-IUPAC samples were used by: +, Aki et al. [27]; △, Kim et al. [48]; ×, Kim et al. [49]; ◇, Shin et al. [50]. The dashed lines represent the approximate combined expanded uncertainties for p(eval) for $x_1 \geq 0.1$. Uncertainties for $x_1 < 0.1$ are shown in Fig. 16.

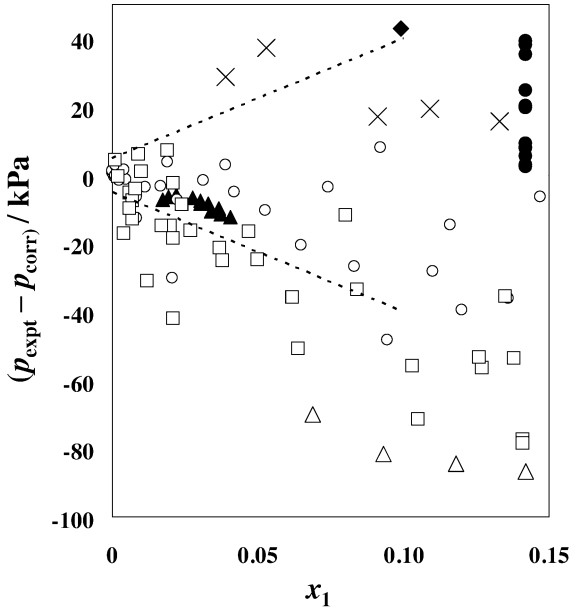

Fig. 16 Deviation plot (absolute deviations) for experimental solubility pressures p from the critically evaluated values p(eval) calculated with eq. 7 for the system {carbon dioxide (1) + $[C_6mim][NTf_2]$ (2)}. The IUPAC sample of $[C_6mim][NTf_2]$ was used by: ◆, Kumelan et al. [31]; ▲, Costa Gomes [44]; ○, Muldoon et al. [45]; □, Shiflett and Yokozeki [46]; ●, Peters and coworkers [47]. Non-IUPAC samples were used by: +, Aki et al. [27]; △, Kim et al. [48]; ×, Kim et al. [49]. The dashed lines represent the approximate combined expanded uncertainties for p(eval) for $x_1 < 0.1$. Uncertainties for $x_1 \geq 0.1$ are shown in Fig. 15.

Table 2 Evaluated solubility pressures p for the system {carbon dioxide (1) + $[C_6mim][NTf_2]$ (2)}.[a]

T/K	x_1[b]	p/MPa
298.15	0.1	(0.35 ± 0.04)
298.15	0.3	(1.30 ± 0.11)
298.15	0.6	(3.81 ± 0.22)
323.15	0.1	(0.52 ± 0.05)
323.15	0.3	(1.95 ± 0.16)
323.15	0.6	(6.15 ± 0.36)
348.15	0.1	(0.72 ± 0.07)
348.15	0.3	(2.74 ± 0.23)
348.15	0.6	(9.22 ± 0.53)

[a]These values are provided as a convenient check for correct implementation of eq. 7 by the reader in a computer program. The full range of validity for eq. 7 is given in the text.
[b]x_1 = the mole fraction of carbon dioxide in the liquid phase.

Vapor–liquid equilibrium studies with other compounds

Other VLE studies involving $[C_6mim][NTf_2]$ have been reported in the literature, but these generally involve unique chemical systems, so no comparisons between results are possible. Studies on mixtures for which the second component is a gas near ambient temperature and pressure include those by Anderson et al. [51] (sulfur dioxide), Costa Gomes [44] (hydrogen, ethane), Kim et al. [49] (propane), Kumelan et al. [52] (methane, xenon), Kumelan et al. [53] (carbon tetrafluoride), Kumelan et al. [54] (hydrogen), Florusse et al. [55] (ethane), Peters and coworkers [47] (carbon monoxide), and Finotello et al. [56] (methane, hydrogen, nitrogen). Studies on mixtures for which the second component is a liquid near ambient temperature and pressure include those by Kato and Gmehling [29] (cyclohexane, cyclohexene, methanol, ethanol), and Nebig et al. [57] (hexane, water).

Activity coefficients of solutes at infinite dilution

Activity coefficients at infinite dilution γ^∞ have been reported for a variety of solutes in $[C_6mim][NTf_2]$ by Kato and Gmehling [29], Letcher et al. [58], Heintz et al. [59], Heintz et al. [60], Shevelyova et al. [61], Dobryakov et al. [62], and Domanska and Marciniak [25]. Only the later study by Heintz et al. [60] involved the IUPAC sample in some measurements. A variety of samples of the ionic liquid were used in the other studies. Nonetheless, the results were found to be consistent (within approximately 5 %) at near the claimed uncertainty levels (typically 3 % with an unspecified level of confidence) for the reported values.

The activity coefficients at infinite dilution γ^∞ were correlated for each binary system studied by more than one research group. Equations representing the results for each of the 20 such chemical systems are included in the Appendix (Table A1). The estimated combined expanded uncertainties ($k = 2$) were estimated to be 7 % for the correlated values. Plots of the experimental and recommended γ^∞ values are included in the Appendix (Figs. A1 to A20).

MIXTURE PROPERTIES (LIQUID–LIQUID EQUILIBRIA)

Liquid–liquid equilibria with water (near pressure $p = 0.1$ MPa)

The solubility of water in the IUPAC sample of $[C_6mim][NTf_2]$ was studied by Chapeaux et al. [63] and Widegren and Magee [4] using coulometric Karl Fischer titration. Additional results for non-IUPAC samples were published earlier by Fitchett et al. [26] and McFarlane et al. [64]. All results are shown in Fig. 17. Results for the IUPAC sample are represented by the following equation:

$$x_{H_2O} = 0.003\,257 \cdot (T/\mathrm{K}) - 0.7529 \tag{9}$$

The temperature range of validity for eq. 9 is $293.15 < (T/\mathrm{K}) < 298.15$. The estimated combined expanded uncertainty ($k = 2$) is 0.01 mole fraction H_2O. Chapeaux et al. [63] also reported the mass fraction solubility of the ionic liquid in water at temperature $T = 296.7$ K: $w = (0.0023 \pm 0.0001)$, which is equivalent to the mole fraction solubility $x = (0.000\,093 \pm 0.000\,004)$.

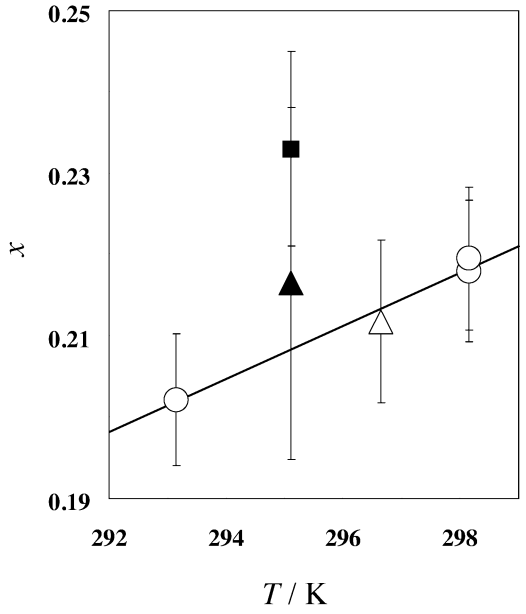

Fig. 17 Mole fraction solubility of water x in [C_6mim][NTf_2] as a function of temperature near pressure p = 0.1 MPa. The error bars represent uncertainty estimates by the authors. ○, Widegren and Magee [4]; △, Chapeaux et al. [63]; ■, Fitchett et al. [26]; ▲, McFarlane et al. [64].

Liquid–liquid equilibria with hexan-1-ol (near pressure p = 0.1 MPa)

LLE temperatures for mixtures of the IUPAC sample of [C_6mim][NTf_2] with hexan-1-ol were reported by Lachwa et al. [21] and Wertz et al. [65]. Earlier measurements with a non-IUPAC sample were reported by Crosthwaite et al. [66]. There is good accord between the various data sets, as shown in Fig. 18. The LLE temperatures T for the measurements involving the IUPAC sample can be represented with the following equation:

$$(T/K) = A_0 + A_1/x_1 + A_2 + x_2 + \sum_{i=3}^{8} A_i \cdot (x_1 - x_2)^i \tag{10}$$

where x_1 and x_2 are the mole fraction of hexan-1-ol and the ionic liquid, respectively. The nine elements of array A are: 340.085, –25.7887, –0.145 647, –70.0321, 472.466, –806.588, –215.847, 1396.47, and –795.781. The range of validity is from x_1 = 0.44 to x_1 = 0.98. The LLE temperature T calculated with this equation for x_1 = 0.700 is (302.99 ± 0.50) K. Deviations from this equation for all data sets are shown in Fig. 19. The estimated combined expanded uncertainty (k = 2) is 0.5 K for $x_1 \leq 0.96$, and increases to 1.5 K for x_1 = 0.98.

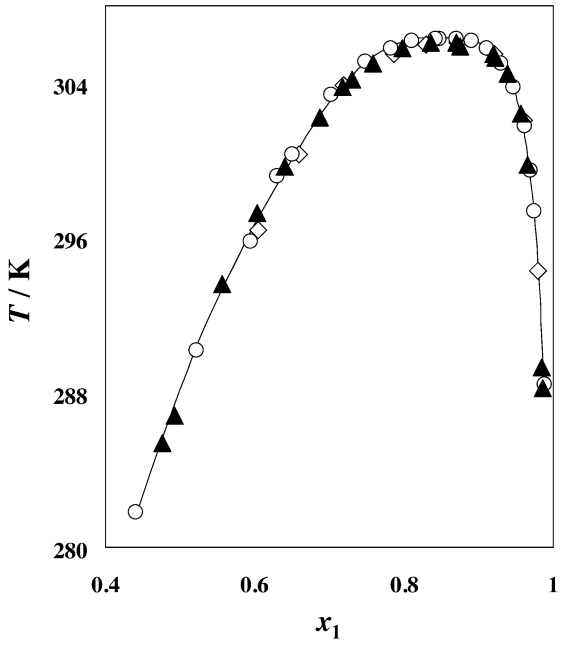

Fig. 18 LLE temperatures T for the system {hexan-1-ol (1) + [C_6mim][NTf_2] (2)}. The line represents the evaluation of this research. The IUPAC sample was studied by: ○, Lachwa et al. [21]; ▲, Wertz et al. [65]. A non-IUPAC sample was studied by: ◇, Crosthwaite et al. [66].

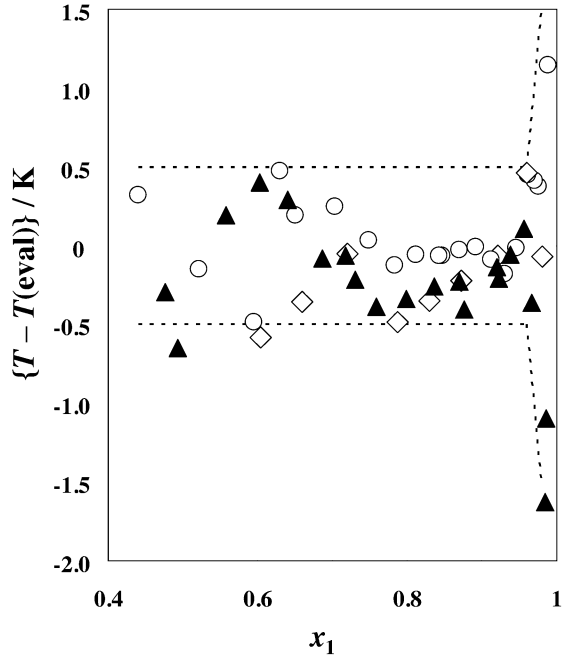

Fig. 19 Deviation plot for experimental LLE temperatures T from the critically evaluated values T(eval) calculated with eq. 10 for the system {hexan-1-ol (1) + [C_6mim][NTf_2] (2)} near $p = 0.1$ MPa. The IUPAC sample was studied by: ○, Lachwa et al. [21]; ▲, Wertz et al. [65]. A non-IUPAC sample was studied by: ◇, Crosthwaite et al. [66]. The dashed lines represent the combined expanded uncertainties for T(eval).

Liquid–liquid equilibria with octan-1-ol (near pressure p = 0.1 MPa)

LLE temperatures for mixtures of the IUPAC sample of [C_6mim][NTf_2] with octan-1-ol were reported by Lachwa et al. [21]. Earlier measurements with a non-IUPAC sample were reported by Crosthwaite et al. [66]. There is good accord between the two data sets, particularly near the consolute composition, as shown in Fig. 20. The measurements involving the IUPAC sample can be represented with eq. 10, where in this case, x_1 is the mole fraction of octan-1-ol. It was found that summation to i = 6 provided an adequate fit to the experimental values. The seven elements of array A are: 364.799, –22.5362, –0.26545, –20.9422, 37.1871, –29.0707, and 3.988 39. The range of validity is from x_1 = 0.281 to x_1 = 0.989. The LLE temperature T calculated with eq. 10 and these parameters for x_1 = 0.600 is (326.46 ± 0.50) K. Deviations from this equation for both data sets are shown in Fig. 21. The estimated combined expanded uncertainty (k = 2) is 0.5 K for $x_1 \leq 0.97$, and increases to 1.5 K for $x_1 > 0.989$.

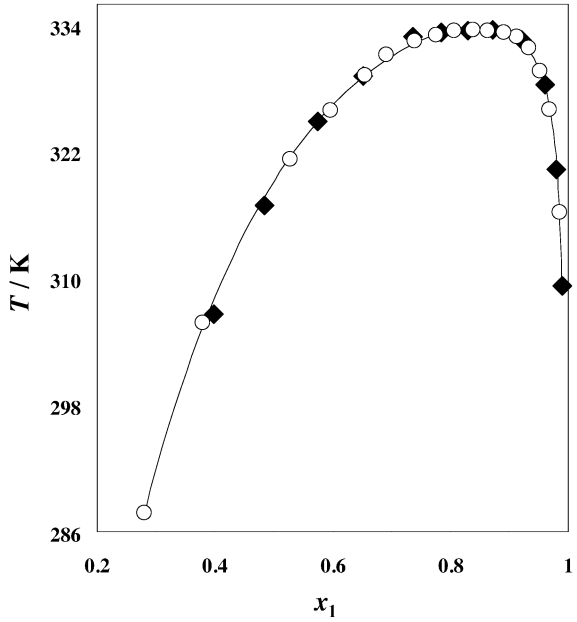

Fig. 20 LLE temperatures T for the system {octan-1-ol (1) + [C_6mim][NTf_2] (2)}. The line represents the evaluation of this research. The IUPAC sample was studied by: ○, Lachwa et al. [21]. A non-IUPAC sample was studied by: ◆, Crosthwaite et al. [66].

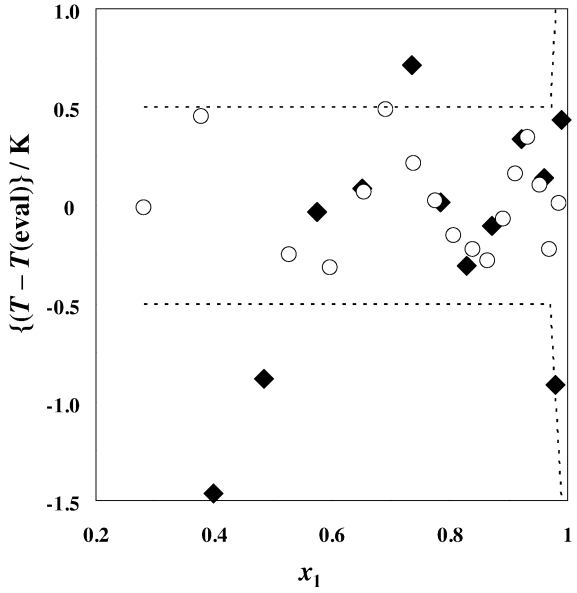

Fig. 21 Deviation plot for experimental LLE temperatures T from the critically evaluated values T(eval) calculated with eq. 10 for the system {octan-1-ol (1) + $[C_6mim][NTf_2]$ (2)} near $p = 0.1$ MPa. The IUPAC sample was studied by: ○, Lachwa et al. [21]. A non-IUPAC sample was studied by: ◆, Crosthwaite et al. [66]. The dashed lines represent the combined expanded uncertainties for T(eval).

MIXTURE PROPERTIES (OTHER PHASE EQUILIBRIA)

Solid–liquid equilibrium involving $[C_6mim][NTf_2]$ was reported by Shevelyova et al. [61] with hexanolactam and cyclohexanone oxime. Recommended values were not generated for these systems.

Shiflett and Yokozeki [46] demonstrated the existence of a region of vapor–liquid–liquid equilibrium for mixtures of CO_2 and $[C_6mim][NTf_2]$ at high concentrations of CO_2 (near $x_{CO_2} = 0.8$). Recently, Shin et al. [50] also reported the observation of LLE near this same high concentration of carbon dioxide. This region of composition is not included in the evaluations reported in this article.

CONCLUSIONS

Thermodynamic, transport, and phase equilibria properties were critically evaluated for $[C_6mim][NTf_2]$ based upon recent measurements made on a carefully prepared and characterized sample. It was shown that good accord between measurements made in different laboratories can be achieved, if careful control of water content of the ionic liquid is maintained. The recommended values provided here are all for the dry ionic liquid and provide benchmark values for property measurements, as well as for sample drying methods and instrument calibration procedures.

ACKNOWLEDGMENTS

For R.D.C., V.D., J.W.M., and M.F. this work represents an official contribution of the U.S. National Institute of Standards and Technology and is not subject to copyright in the United States.

REFERENCES

1. <http://www.iactweb.org/>. Accessed 20 January 2009.
2. P. Wassersheid, T. Welton (Eds.). *Ionic Liquids in Synthesis*, 2 Vols., Wiley-VCH, Weinheim (2007).
3. K. N. Marsh, J. F. Brennecke, R. D. Chirico, M. Frenkel, A. Heintz, J. W. Magee, C. J. Peters, L. P. N. Rebelo, K. R. Seddon. *Pure Appl. Chem.* **81**, 781 (2009).
4. J. A. Widegren, J. W. Magee. *J. Chem. Eng. Data* **52**, 2331 (2007).
5. A. V. Blokhin, Y. U. Paulechka, G. J. Kabo. *J. Chem. Eng. Data* **51**, 1377 (2006).
6. V. V. Diky, R. D. Chirico, R. C. Wilhoit, Q. Dong, M. Frenkel. *J. Chem. Inf. Comput. Sci.* **43**, 15 (2003).
7. M. Frenkel, Q. Dong, R. C. Wilhoit, K. R. Hall. *Int. J. Thermophys*. **22**, 215 (2001).
8. X. Yan, Q. Dong, M. Frenkel, K. R. Hall. *Int. J. Thermophys.* **22**, 227 (2001).
9. (a) M. Frenkel, R. D. Chirico, V. Diky, X. Yan, Q. Dong, C. Muzny. *J. Chem. Inf. Model.* **45**, 816 (2005); (b) V. Diky, C. D. Muzny, E. W. Lemmon, R. D. Chirico, M. Frenkel. *J. Chem. Inf. Model.* **47***,* 1713 (2007).
10. (a) M. Frenkel, R. D. Chirico, V. Diky, X. Yan, Q. Dong, C. Muzny. *NIST ThermoData Engine, NIST Standard Reference Database 103a*, *Version 2.1;* National Institute of Standards and Technology, Standard Reference Data Program, Gaithersburg, MD (2008); (b) M. Frenkel, R. D. Chirico, V. Diky, C. D. Muzny, A. F. Kazakov, E. W. Lemmon. *NIST ThermoData Engine, NIST Standard Reference Database 103b*, *Version 3.0*, National Institute of Standards and Technology, Standard Reference Data Program: Gaithersburg, MD (2008).
11. *Guide to the Expression of Uncertainty in Measurement* (International Organization for Standardization, Geneva, Switzerland, 1993). This *Guide* was prepared by ISO Technical Advisory Group 4 (TAG 4), Working Group 3 (WG 3). ISO/TAG 4 has as its sponsors the BIPM (Bureau International des Poids et Mesures), IEC (International Electrotechnical Commission), IFCC (International Federation of Clinical Chemistry and Laboratory Medicine), ISO, IUPAC (International Union of Pure and Applied Chemistry), IUPAP (International Union of Pure and Applied Physics), and OIML (Organisation Internationale de Métrologie Légale). Although the individual members of WG 3 were nominated by the BIPM, IEC, ISO, or OIML, the *Guide* is published by ISO in the name of all seven organizations.
12. B. N. Taylor, C. E. Kuyatt. *Guidelines for the Evaluation and Expression of Uncertainty in NIST Measurement Results*, NIST Technical Note 1297, National Institute of Standards and Technology, Gaithersburg, MD (1994). <http://physics.nist.gov/cuu/Uncertainty/bibliography.html/>. Accessed 20 January 2009.
13. R. D. Chirico, M. Frenkel, V. V. Diky, K. N. Marsh, R. C. Wilhoit. *J. Chem. Eng. Data* **48**, 1344 (2003).
14. Y. Shimizu, Y. Ohte, Y. Yamamura, K. Saito, T. Atake. *J. Phys. Chem. B* **110**, 13970 (2006).
15. D. G. Archer. National Institute of Standards and Technology, Investigation Report-6645, Gaithersburg, MD (2006).
16. J. M. Crosthwaite, M. J. Muldoon, J. K. Dixon, J. L. Anderson, J. F. Brennecke. *J. Chem. Thermodyn.* **37**, 559 (2005).
17. H. Tokuda, K. Hayamizu, K. Ishii, M. A. B. H. Susan, M. Watanabe. *J. Phys. Chem. B* **109**, 6103 (2005).
18. Q. Dong, R. D. Chirico, X. Yan, X. Hong, M. Frenkel. *J. Chem. Eng. Data* **50**, 546 (2005).
19. A. Diedrichs, J. Gmehling. *Fluid Phase Equilibr.* **244**, 68 (2006).
20. R. Ge, C. Hardacre, J. Jacquemin, P. Nancarrow, D. W. Rooney. *J. Chem. Eng. Data* **53**, 2148 (2008).
21. J. Lachwa, P. Morgado, J. M. S. S. Esperanca, H. J. R. Guedes, J. N. C. Lopes, L. P. N. Rebelo. *J. Chem. Eng. Data* **51**, 2215 (2006).

22. M. E. Kandil, K. N. Marsh, A. R. H. Goodwin. *J. Chem. Eng. Data* **52**, 2382 (2007).
23. J. M. S. S. Esperanca, H. J. R. Guedes, J. N. C. Lopes, L. P. N. Rebelo. *J. Chem. Eng. Data* **53**, 867 (2008).
24. K. R. Seddon, G. Driver. Personal communication.
25. U. Domanska, A. Marciniak. Personal communication.
26. B. D. Fitchett, T. N. Knepp, J. C. Conboy. *J. Electrochem. Soc.* **151**, E219 (2004).
27. S. N. V. K. Aki, B. R. Mellein, E. M. Saurer, J. F. Brennecke. *J. Phys. Chem. B* **108**, 20355 (2004).
28. R. Gomes de Azevedo, J. M. S. S. Esperanca, J. Szydlowski, Z. P. Visak, P. F. Pires, H. J. R. Guedes, L. P. N. Rebelo. *J. Chem. Thermodyn*. **37**, 888 (2005).
29. R. Kato, J. Gmehling. *J. Chem. Thermodyn.* **37**, 603 (2005).
30. J. N. C. Lopes, T. C. Cordeiro, J. M. S. S. Esperanca, H. J. R. Guedes, S. Huq, L. P. N. Rebelo, K. R. Seddon. *J. Phys. Chem.* **109**, 3519 (2005).
31. J. Kumelan, A. P.-S. Kamps, D. Tuma, G. Maurer. *J. Chem. Thermodyn.* **38**, 1396 (2006).
32. H. Tokuda, S. Tsuzuki, M. A. B. H. Susan, K. Hayamizu, M. Watanabe. *J. Phys. Chem. B* **110**, 19593 (2006).
33. A. Muhammad, M. I. A. Mutalib, C. D. Wilfred, T. Murugesan, A. Shafeeq. *J. Chem. Thermodyn.* **40**, 1433 (2008)
34. D. H. Zaitsau, G. J. Kabo, A. A. Strechan, Y. U. Paulechka, A. Tschersich, S. P. Verevkin, A. Heintz. *J. Phys. Chem. A* **110**, 7303 (2006).
35. F. J. V. Santos, A. P. Ribeiro, C. Nieto de Castro. Asian Thermophysical Properties Conference, Fukuoka, Japan, 21–24 August, Paper No. 263 (2007).
36. A. Ahosseini, A. M. Scurto. *Int. J. Thermophys*. **29**, 1222 (2008).
37. J. A. Widegren, E. M. Saurer, K. N. Marsh, J. W. Magee. *J. Chem. Thermodyn.* **37**, 569 (2005).
38. C. Frez, G. J. Diebold, C. D. Tran, S. Yu. *J. Chem. Eng. Data* **51**, 1250 (2006).
39. J. Hunger, A. Stoppa, G. Hefter, R. Buchner. Published in ref. [3].
40. P. Kilaru, G. A. Baker, P. Scovazzo. *J. Chem. Eng. Data* **52**, 2306 (2007).
41. P. J. Carvalho, M. G. Freire, I. M. Marrucho, A. J. Queimada. *J. Chem. Eng. Data* **53**, 1346 (2008).
42 U. Domanska, A. Marciniak. Personal communication.
43. R. Ge, C. Hardacre, P. Nancarrow, D. W. Rooney. *J. Chem. Eng. Data* **52**, 1819 (2007).
44. M. F. Costa Gomes. *J. Chem. Eng. Data* **52**, 472 (2007).
45. M. J. Muldoon, S. N. V. K. Aki, J. L. Anderson, J. K. Dixon, J. F. Brennecke. *J. Phys. Chem. B* **111**, 9001 (2007).
46. M. B. Shiflett, A. Yokozeki. *J. Phys. Chem. B* **111**, 2070 (2007).
47. C. J. Peters et al. Personal communication.
48. Y. S. Kim, W. Y. Choi, J. H. Jang, K. P. Yoo, C. S. Lee. *Fluid Phase Equilibr.* **228–229**, 439 (2005).
49. Y. S. Kim, J. H. Jang, B. D. Lim, J. W. Kang, C. S. Lee. *Fluid Phase Equilibr*. **256**, 70 (2007).
50. E.-K. Shin, B.-C. Lee, J. S. Lim. *J. Supercrit. Fluids* **45**, 282 (2008).
51. J. L. Anderson, J. K. Dixon, E. J. Maginn, J. F. Brennecke. *J. Phys. Chem. B* **110**, 15059 (2006).
52. J. Kumelan, A. P.-S. Kamps, D. Tuma, G. Maurer. *Ind. Eng. Chem. Res.* **46**, 8236 (2007).
53. J. Kumelan, A. P.-S. Kamps, D. Tuma, A. Yokozeki, M. B. Shiflett, G. Maurer. *J. Phys. Chem. B* **112**, 3040 (2008).
54. J. Kumelan, A. P.-S. Kamps, D. Tuma, G. Maurer. *J. Chem. Eng. Data* **51**, 434 (2006).
55. J. J. Florusse, S. Raeissi, C. J. Peters. *J. Chem. Eng. Data* **53**, 1283 (2008).
56. A. Finotello, J. E. Bara, D. Camper, R. D. Noble. *Ind. Eng. Chem. Res.* **47**, 3453 (2008).
57. S. Nebig, R. Bolts, J. Gmehling. *Fluid Phase Equilibr.* **258**, 168 (2007).
58. T. M. Letcher, A. Marciniak, M. Marciniak, U. Domanska. *J. Chem. Thermodyn.* **37**, 1327 (2005).
59. A. Heintz, S. P. Verevkin, D. Ondo. *J. Chem. Eng. Data* **51**, 648 (2006).

60. A. Heintz, S. P. Verevkin, J. K. Lehmann, T. V. Vasiltsova, D. Ondo. *J. Chem. Thermodyn.* **39**, 268 (2007).
61. M. P. Shevelyova, D. H. Zaitsau, Y. U. Paulechka, A. V. Blokhin, G. J. Kabo. *J. Chem. Eng. Data* **52**, 1360 (2007).
62. Y. G. Dobryakov, D. Tuma, G. Maurer. *J. Chem. Eng. Data* **53**, 2154 (2008).
63. A. Chapeaux, L. D. Simoni, M. A. A. Stadtherr, J. F. Brennecke. *J. Chem. Eng. Data* **52**, 2467 (2007).
64. J. McFarlane, W. B. Ridenour, H. Luo, R. D. Hunt, D. W. DePaoli. *Sep. Sci. Technol.* **40**, 1245 (2005).
65. C. Wertz, A. Tschersich, J. K. Lehmann, A. Heintz. *J. Mol. Liq.* **131–132**, 2 (2007).
66. J. M. Crosthwaite, S. N. V. K. Aki, E. J. Maginn, J. F. Brennecke. *Fluid Phase Equilibr.* **228–229**, 303 (2005).

APPENDIX: ACTIVITY COEFFICIENTS AT INFINITE DILUTION

Table A1 Activity coefficients at infinite dilution γ^{∞} for solutes in $[C_6mim][NTf_2]$.[a]

Solute	References	γ^{∞} Representation	Range of validity/K
pentane	[29,58,59]	$17.14 - 3.614\cdot10^{-2}\cdot(T/K)$	298 to 344
hexane	[29,58,59]	$18.39 - 3.419\cdot10^{-2}\cdot(T/K)$	298 to 344
heptane	[29,58,59]	$26.76 - 5.215\cdot10^{-2}\cdot(T/K)$	298 to 344
octane	[29,58,59]	$37.86 - 7.629\cdot10^{-2}\cdot(T/K)$	298 to 344
cyclopentane	[29,58]	$8.46 - 1.536\cdot10^{-2}\cdot(T/K)$	298 to 333
cyclohexane	[29,58,59]	$13.19 - 2.569\cdot10^{-2}\cdot(T/K)$	298 to 333
pent-1-ene	[29,59]	$5.35 - 6.154\cdot10^{-3}\cdot(T/K)$	302 to 333
hex-1-ene	[29,58,59]	$8.61 - 1.301\cdot10^{-2}\cdot(T/K)$	298 to 344
hept-1-ene	[29,59]	$12.70 - 2.085\cdot10^{-2}\cdot(T/K)$	302 to 354
oct-1-ene	[29,58,59]	$16.78 - 2.730\cdot10^{-2}\cdot(T/K)$	298 to 354
cyclohexene	[29,59]	$6.76 - 1.128\cdot10^{-2}\cdot(T/K)$	302 to 344
benzene	[29,58,59]	$0.56 + 6.155\cdot10^{-4}\cdot(T/K)$	298 to 344
toluene	[29,59]	$0.55 + 1.548\cdot10^{-3}\cdot(T/K)$	303 to 344
methanol	[25,29,58,59,60,62]	$10.89 - 5.031\cdot10^{-2}\cdot(T/K) + 6.251\cdot10^{-5}\cdot(T/K)^2$	293 to 354
ethanol	[29,59,62]	$11.72 - 5.040\cdot10^{-2}\cdot(T/K) + 5.722\cdot10^{-5}\cdot(T/K)^2$	293 to 354
propan-1-ol	[29,59,62]	$7.18 - 1.991\cdot10^{-2}\cdot(T/K) + 8.579\cdot10^{-6}\cdot(T/K)^2$	293 to 354
propan-2-ol	[29,59,62]	$19.94 - 9.971\cdot10^{-2}\cdot(T/K) + 1.310\cdot10^{-4}\cdot(T/K)^2$	293 to 354
butan-1-ol	[25,59,60,62]	$15.08 - 6.385\cdot10^{-2}\cdot(T/K) + 7.173\cdot10^{-5}\cdot(T/K)^2$	293 to 386
hexan-1-ol	[25,59,60]	$22.89 - 9.996\cdot10^{-2}\cdot(T/K) + 1.166\cdot10^{-4}\cdot(T/K)^2$	298 to 396
acetone	[29,59]	$0.12 + 7.112\cdot10^{-4}\cdot(T/K)$	302 to 354

[a]Only solutes for which more than one study was completed are listed.

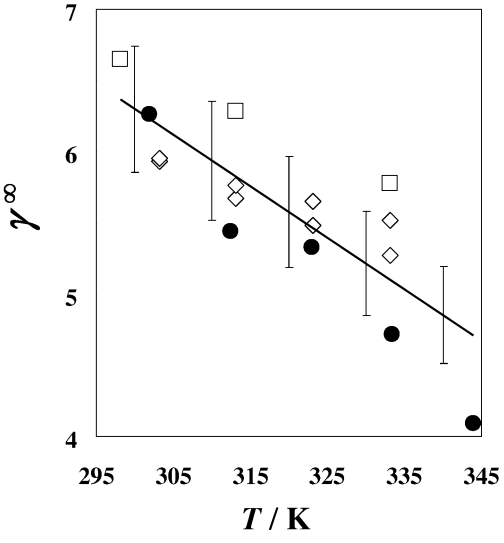

Fig. A1 Activity coefficient at infinite dilution γ^{∞} for pentane in $[C_6mim][NTf_2]$. The line represents the fit to the experimental values. The equation for the line is given in Table 2. The error bars represent approximately $0.07\cdot\gamma^{\infty}$. ◇, Kato and Gmehling [29]; □, Letcher et al. [58]; ●, Heintz et al. [59].

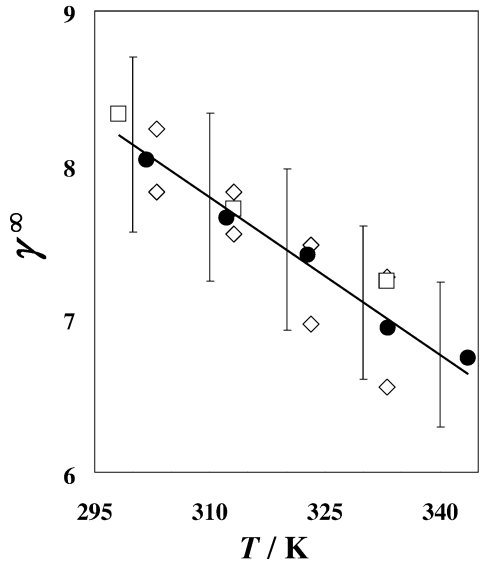

Fig. A2 Activity coefficient at infinite dilution γ^∞ for hexane in [C_6mim][NTf_2]. The line represents the fit to the experimental values. The equation for the line is given in Table A1. The error bars represent approximately 0.07·γ^∞. ◇, Kato and Gmehling [29]; □, Letcher et al. [58]; ●, Heintz et al. [59].

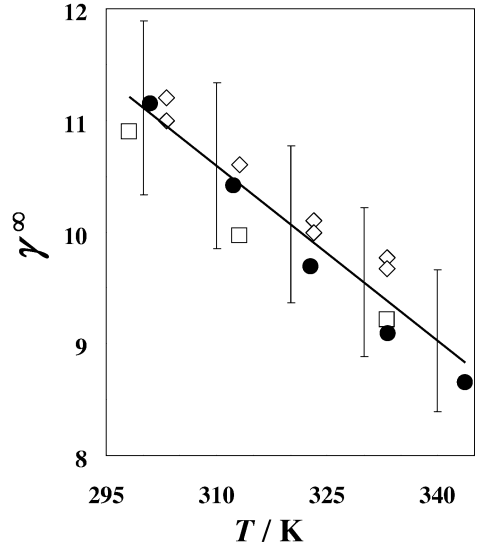

Fig. A3 Activity coefficient at infinite dilution γ^∞ for heptane in [C_6mim][NTf_2]. The line represents the fit to the experimental values. The equation for the line is given in Table A1. The error bars represent approximately 0.07·γ^∞. ◇, Kato and Gmehling [29]; □, Letcher et al. [58]; ●, Heintz et al. [59].

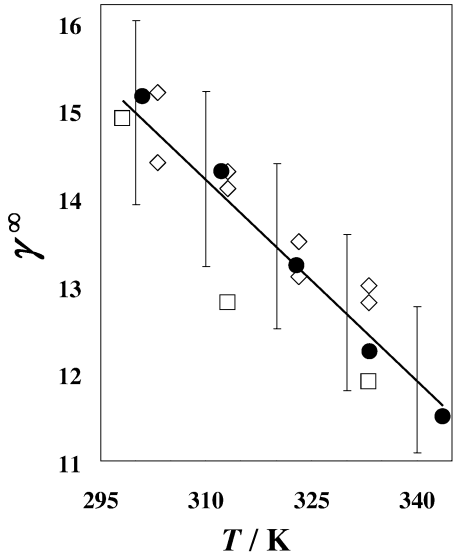

Fig. A4 Activity coefficient at infinite dilution γ^{∞} for octane in $[C_6mim][NTf_2]$. The line represents the fit to the experimental values. The equation for the line is given in Table A1. The error bars represent approximately $0.07 \cdot \gamma^{\infty}$. ◇, Kato and Gmehling [29]; □, Letcher et al. [58]; ●, Heintz et al. [59].

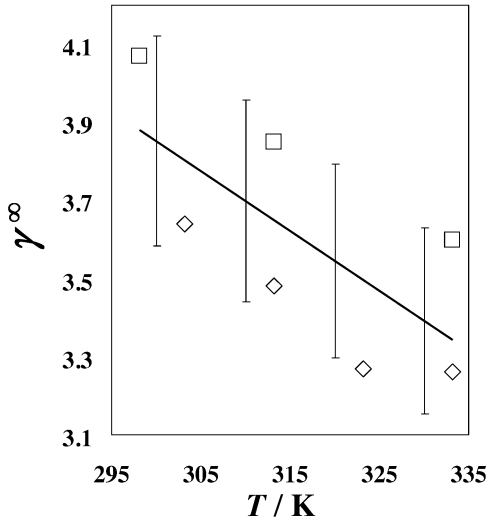

Fig. A5 Activity coefficient at infinite dilution γ^{∞} for cyclopentane in $[C_6mim][NTf_2]$. The line represents the fit to the experimental values. The equation for the line is given in Table A1. The error bars represent approximately $0.07 \cdot \gamma^{\infty}$. ◇, Kato and Gmehling [29]; □, Letcher et al. [58].

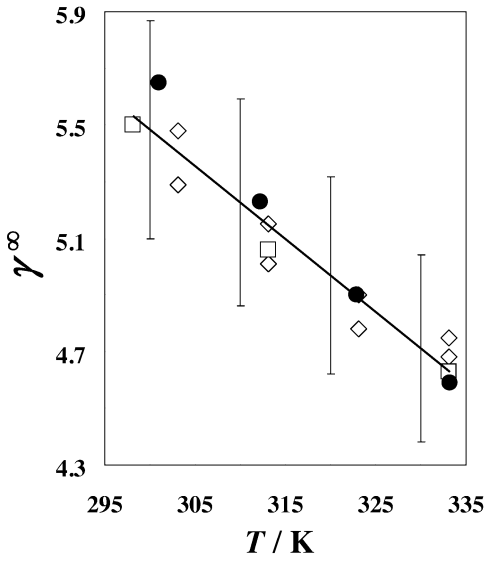

Fig. A6 Activity coefficient at infinite dilution γ^{∞} for cyclohexane in $[C_6mim][NTf_2]$. The line represents the fit to the experimental values. The equation for the line is given in Table A1. The error bars represent approximately $0.07 \cdot \gamma^{\infty}$. ◇, Kato and Gmehling [29]; □, Letcher et al. [58]; ●, Heintz et al. [59].

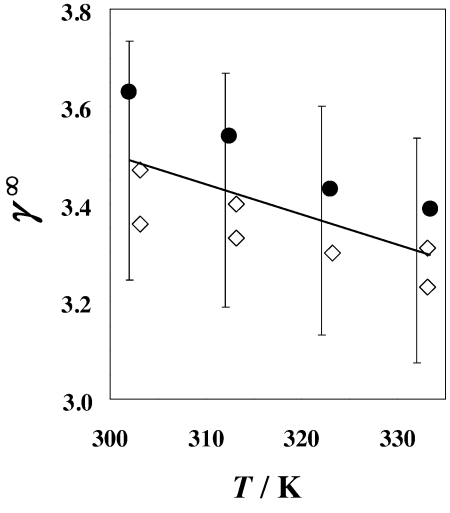

Fig. A7 Activity coefficient at infinite dilution γ^{∞} for pent-1-ene in $[C_6mim][NTf_2]$. The line represents the fit to the experimental values. The equation for the line is given in Table A1. The error bars represent approximately $0.07 \cdot \gamma^{\infty}$. ◇, Kato and Gmehling [29]; ●, Heintz et al. [59]. (A typographical error in ref. [59] was corrected here. Temperatures corresponding to the γ^{∞} values were accidentally inverted (highest to lowest) in the original publication.)

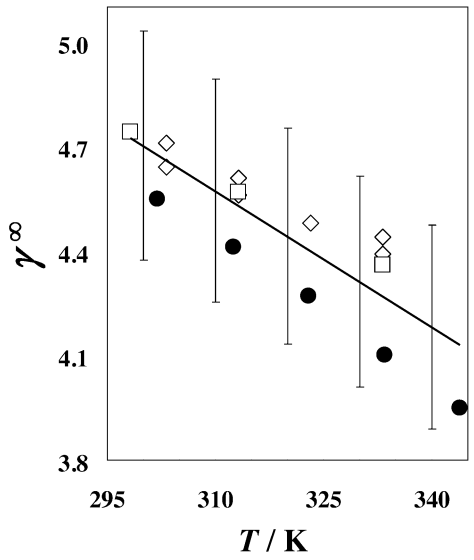

Fig. A8 Activity coefficient at infinite dilution γ^{∞} for hex-1-ene in [C_6mim][NTf_2]. The line represents the fit to the experimental values. The equation for the line is given in Table A1. The error bars represent approximately $0.07 \cdot \gamma^{\infty}$. ◇, Kato and Gmehling [29]; □, Letcher et al. [58]; ●, Heintz et al. [59].

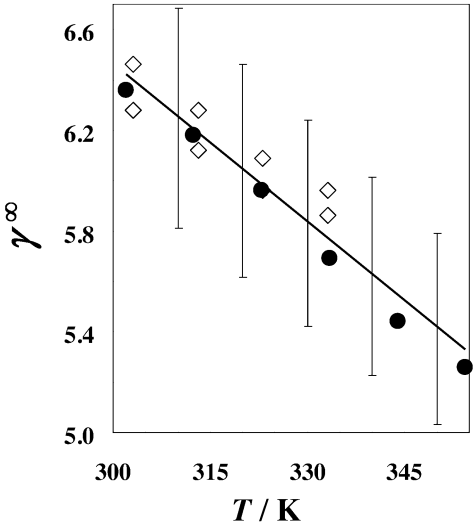

Fig. A9 Activity coefficient at infinite dilution γ^{∞} for hept-1-ene in [C_6mim][NTf_2]. The line represents the fit to the experimental values. The equation for the line is given in Table A1. The error bars represent approximately $0.07 \cdot \gamma^{\infty}$. ◇, Kato and Gmehling [29]; ●, Heintz et al. [59].

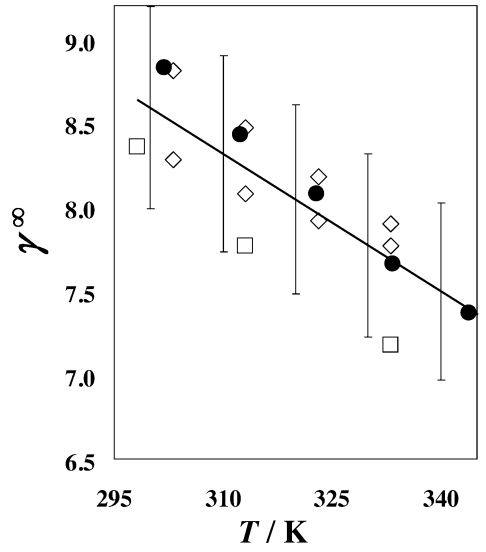

Fig. A10 Activity coefficient at infinite dilution γ^∞ for oct-1-ene in $[C_6mim][NTf_2]$. The line represents the fit to the experimental values. The equation for the line is given in Table A1. The error bars represent approximately $0.07 \cdot \gamma^\infty$. ◇, Kato and Gmehling [29]; □, Letcher et al. [58]; ●, Heintz et al. [59].

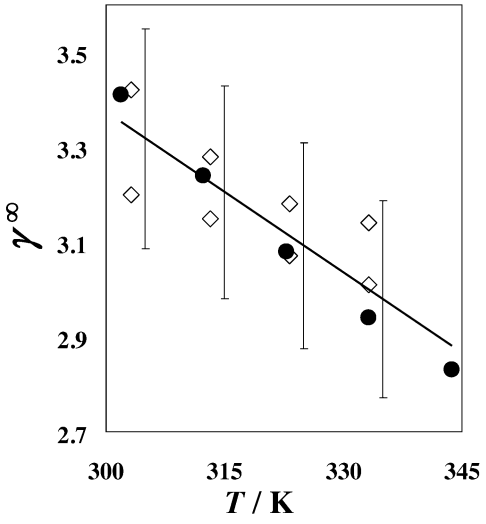

Fig. A11 Activity coefficient at infinite dilution γ^∞ for cyclohexene in $[C_6mim][NTf_2]$. The line represents the fit to the experimental values. The equation for the line is given in Table A1. The error bars represent approximately $0.07 \cdot \gamma^\infty$. ◇, Kato and Gmehling [29]; ●, Heintz et al. [59].

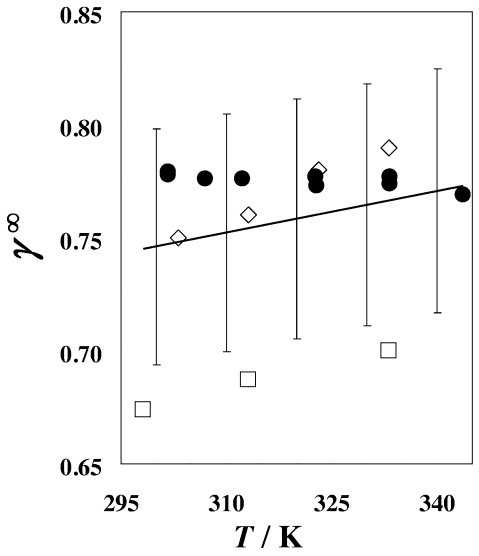

Fig. A12 Activity coefficient at infinite dilution γ^{∞} for benzene in [C_6mim][NTf_2]. The line represents the fit to the experimental values. The equation for the line is given in Table A1. The error bars represent approximately 0.07·γ^{∞}. ◇, Kato and Gmehling [29]; □, Letcher et al. [58]; ●, Heintz et al. [59].

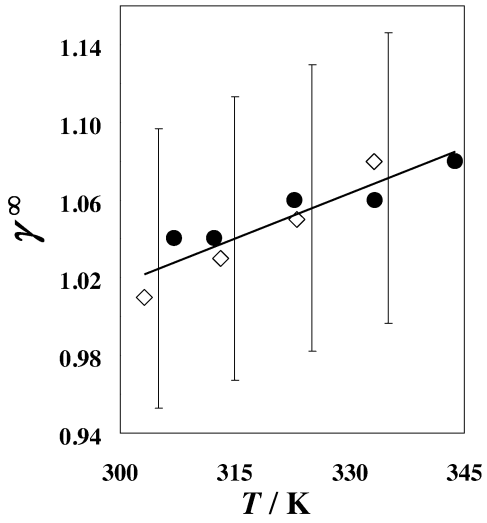

Fig. A13 Activity coefficient at infinite dilution γ^{∞} for toluene in [C_6mim][NTf_2]. The line represents the fit to the experimental values. The equation for the line is given in Table A1. The error bars represent approximately 0.07·γ^{∞}. ◇, Kato and Gmehling [29]; ●, Heintz et al. [59].

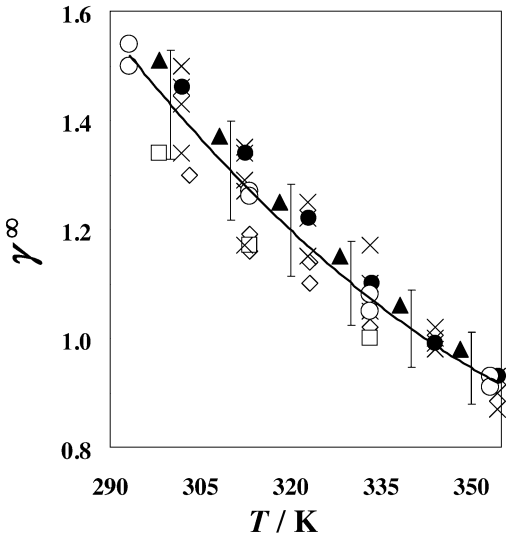

Fig. A14 Activity coefficient at infinite dilution γ^{∞} for methanol in $[C_6mim][NTf_2]$. The line represents the fit to the experimental values. The equation for the line is given in Table A1. The error bars represent approximately $0.07 \cdot \gamma^{\infty}$. ▲, Domanska and Marciniak [25]; ◇, Kato and Gmehling [29]; □, Letcher et al. [58]; ●, Heintz et al. [59]; ×, Heintz et al. [60]; ○, Dobryakov et al. [62].

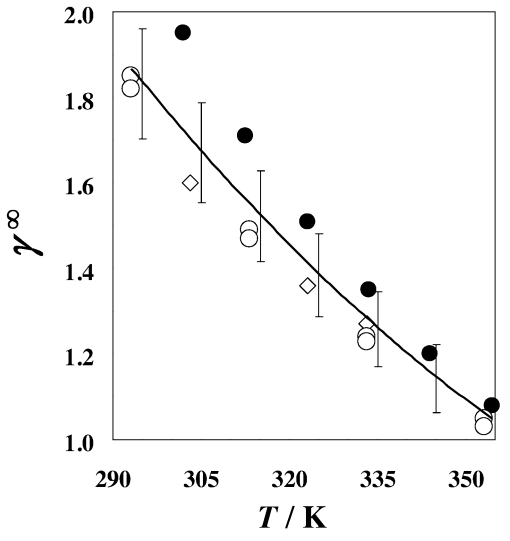

Fig. A15 Activity coefficient at infinite dilution γ^{∞} for ethanol in $[C_6mim][NTf_2]$. The line represents the fit to the experimental values. The equation for the line is given in Table A1. The error bars represent approximately $0.07 \cdot \gamma^{\infty}$. ◇, Kato and Gmehling [29]; ●, Heintz et al. [59]; ○, Dobryakov et al. [62].

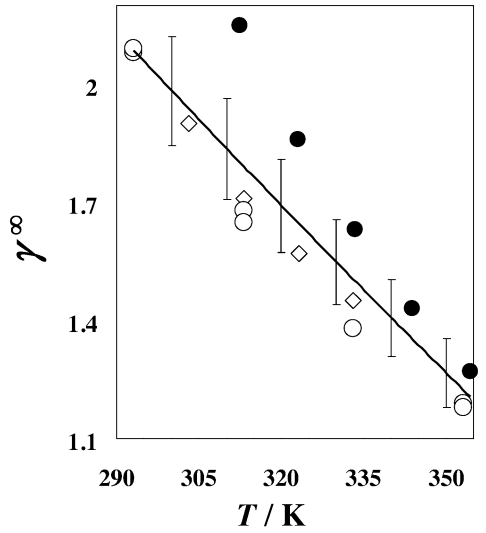

Fig. A16 Activity coefficient at infinite dilution γ^{∞} for propan-1-ol in $[C_6mim][NTf_2]$. The line represents the fit to the experimental values. The equation for the line is given in Table A1. The error bars represent approximately $0.07 \cdot \gamma^{\infty}$. ◇, Kato and Gmehling [29]; ●, Heintz et al. [59]; ○, Dobryakov et al. [62].

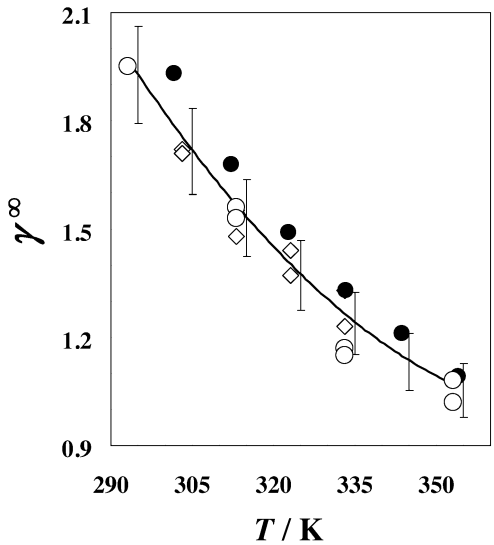

Fig. A17 Activity coefficient at infinite dilution γ^{∞} for propan-2-ol in $[C_6mim][NTf_2]$. The line represents the fit to the experimental values. The equation for the line is given in Table A1. The error bars represent approximately $0.07 \cdot \gamma^{\infty}$. ◇, Kato and Gmehling [29]; ●, Heintz et al. [59]; ○, Dobryakov et al. [62].

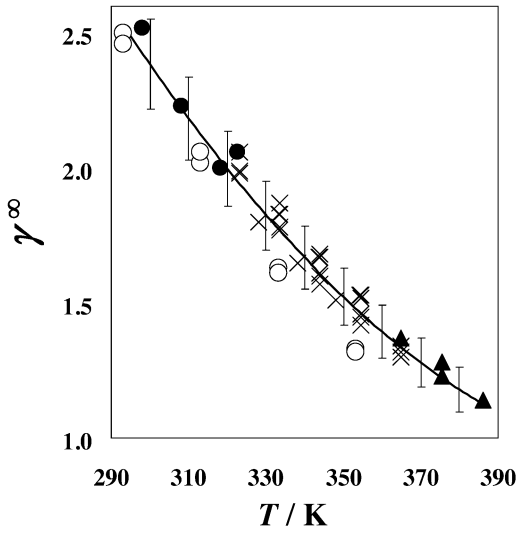

Fig. A18 Activity coefficient at infinite dilution γ^{∞} for butan-1-ol in $[C_6mim][NTf_2]$. The line represents the fit to the experimental values. The equation for the line is given in Table A1. The error bars represent approximately $0.07 \cdot \gamma^{\infty}$. ▲, Domanska and Marciniak [29]; ●, Heintz et al. [59]; ×, Heintz et al. [60]; ○, Dobryakov, et al. [62].

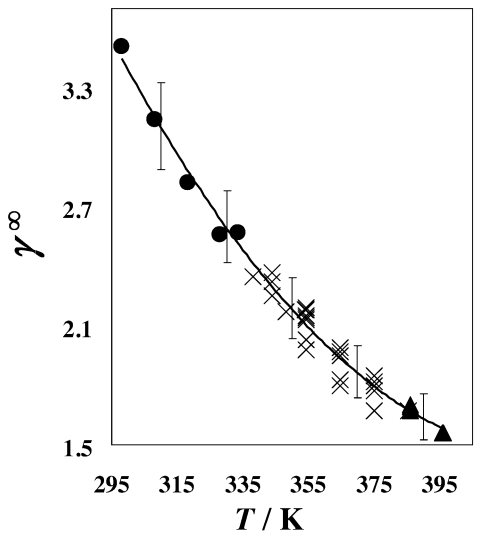

Fig. A19 Activity coefficient at infinite dilution γ^{∞} for hexan-1-ol in $[C_6mim][NTf_2]$. The line represents the fit to the experimental values. The equation for the line is given in Table A1. The error bars represent approximately $0.07 \cdot \gamma^{\infty}$. ▲, Domanska and Marciniak [29]; ●, Heintz et al. [59]; ×, Heintz et al. [60].

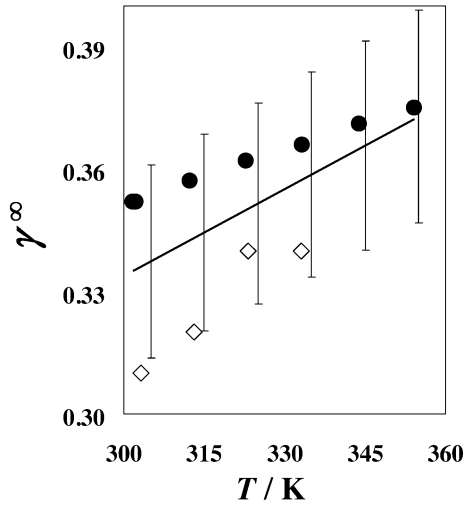

Fig. A20 Activity coefficient at infinite dilution γ^{∞} for acetone in [C_6mim][NTf_2]. The line represents the fit to the experimental values. The equation for the line is given in Table A1. The error bars represent approximately $0.07 \cdot \gamma^{\infty}$. ◇, Kato and Gmehling [29]; ●, Heintz et al. [59].